ANALYSIS AND OPTIMIZATION OF A CRASHWORTHY HELICOPTER SEAT

by

MHASKAR NAUMAN HASAN ABDUL LATIF

Presented to the Faculty of the Graduate School of

The University of Texas at Arlington in Partial Fulfillment

of the Requirements

for the Degree of

MASTER OF SCIENCE IN MECHANICAL ENGINEERING

THE UNIVERSITY OF TEXAS AT ARLINGTON

May 2008

ACKNOWLEDGEMENTS

I would like to express my deep sense of gratitude to my esteemed advisor Dr. Kent Lawrence, for his patience, guidance and assistance during my thesis work. This thesis would not have been possible without his unlimited support and encouragement and I am indebted to him for the unconditional support that he provided during difficult times encountered.

I would also like to mention a special thanks to Dr. Wen S. Chan and Dr. B. P. Wang for helping me clear my doubts whenever required, and also for serving as members on my committee.

March 14, 2008

ABSTRACT

ANALYSIS AND OPTIMIZATION OF A CRASHWORTHY

HELICOPTER SEAT

Nauman Mhaskar, M.S.

The University of Texas at Arlington, 2008

Supervising Professor: Dr. Kent L. Lawrence

The objective of a crashworthy seat is to improve the survivability of occupants (cockpit and cabin) in helicopter crashes. All modern helicopter seats are equipped with an energy absorber to reduce lumbar spine load during crash landing. The main objective of this research is to carry out the structural analysis and optimization of a helicopter crashworthy troop seat assembly using finite element methods. The transient dynamic nonlinear finite element analysis helps in identifying whether the seat structure survives in a crash landing situation, and optimization helps in reducing the weight of the crashworthy seat.

The seat is analyzed using a combination of MATLAB and the Flexible dynamic module of ANSYS Workbench 11.0, while the optimization will be carried out using Design of Experiments from inbuilt ANSYS DesignXplorer.

The analysis points out the weakest links in the crashworthy seat structure and optimization is then carried to make it failsafe as well as reduce the weight of the assembly.

TABLE OF CONTENTS

LIST OF FIGURES

LIST OF TABLES

CHAPTER 1

INTRODUCTION

1.1 The Need for a Crashworthy Helicopter Seat

"The unique flight capabilities of a helicopter permit it to engage in missions that are virtually impossible for any fixed-wing aircraft. Primary among these is the helicopter's ability to hover as well as its capacity to land on any flat terrain without a runway, fly ultra-slowly, or even into reverse, and vertically climb or descend quickly" [1].

"The unique flight missions of helicopters tend to stretch both the aircraft performance as well as the pilot's operational capability thus making them very difficult to fly. They are inherently unstable aircraft with a significant delay in the response time from the pilot control inputs. Helicopter pilots must learn to anticipate wind effect and gust load conditions and compensate for them in advance. The typical helicopter flight mission places an already difficult-to-fly aircraft into an even more difficult and hazardous environment" [1].

Over the 8-year period from 1995 to 2002, 459 [1] workers were killed in incidents involving helicopters, according to data from the Bureau of Labor Statistics (BLS) Census of Fatal Occupational Injuries (CFOI) [1]. Nearly half (47 percent) of those killed in such incidents, worked in government, including 150 in the resident armed forces [1]. The number of fatalities involving helicopters reached a high of 76 in 1998 and declined steadily thereafter to a low of 37 in 2002 (Table 1.1).

Table 1.1: Number of fatalities (Ref 1)

Year	# Fatalities
1995	50
1996	70
1997	64

Table 1.1 - Continued

1998	76
1999	50
2000	69
2001	43
2002	37

Although the number of this type of fatal work injury has declined in recent years, such incidents continue to present an occupational health challenge.

The objective of a crashworthy seat is to improve the survivability of occupants (cockpit and cabin) in helicopter crashes. All modern helicopter seats are equipped with an energy absorber to reduce lumbar spine load during crash landing. The U.S. Army's introduction of armored energy-absorbing crashworthy crew-seats in the UH-60A Black Hawk in the late 1970's ushered in a new era of aviator protection. The energy absorption characteristics of these seats have been demonstrated repeatedly in high-energy ground impacts in which injuries were prevented and/or lives were saved [2].

“Spinal injury may be one of the most serious injuries during aircraft emergency landing and/or pilot ejection from a disabled aircraft. A human’s tolerance to impact acceleration is a function of the energy transferred to the body by the impact, or the work done by the impact. A human's tolerance to impact forces is affected by several variables, including age, sex, general state of health, and an occupant's position in a seat. Federal Aviation Regulations use the load transferred to the spine in determining the probability of a spinal injury” [3]. “During the impact phase, when the occupant and aircraft decelerate, the life-threatening mechanism is the dissipation of the occupant’s kinetic energy. This transfer of energy out of the body appears in the form of relative velocities between body parts and between the body parts and the aircraft.

Due to the transient nature of relative velocities, these body parts experience relative accelerations". [2]

The relative accelerations create forces in the segments that connect body parts. Injury occurs as the forces between body parts exceed the strength of the connecting segments. Due to the structure of the human body, acceleration along the occupant spinal axis is the principal cause of injury during impact [2].

Damage to the vertebral column, particularly the upper lumbar and lower thoracic regions, occurs frequently in positive G impact, where the force is directed parallel to the spine. If some form of energy absorption mechanism is not adopted, the lumbar spine load will exceed its restrictive criterion of 6.67 kN [4] causing permanent injuries or even a fatality. The reduction of these injurious decelerations to non-injurious levels is accomplished by allowing the occupant to displace relative to the impact surface when his/her deceleration level exceeds a specified value [4].

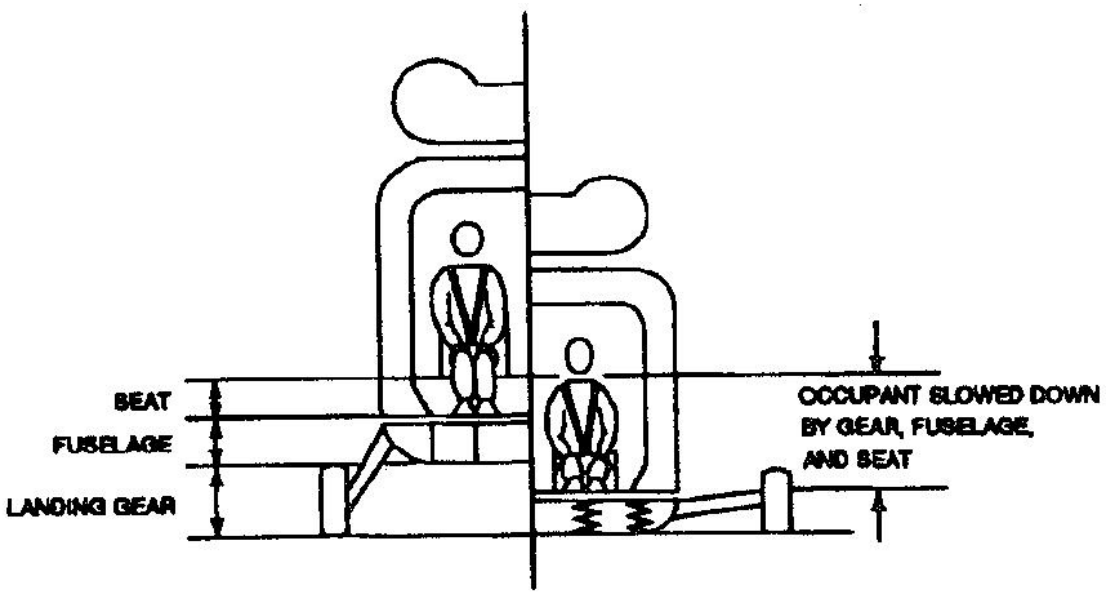

Figure 1.1: Crash energy absorption components (Ref 5)

Occupants involved in helicopter crashes in which the structural integrity of the airframe is maintained, may sustain disabling injuries unless some form of occupant energy protection is

provided. These injuries can reduce the probability of a successful rescue. Energy absorption in a helicopter crash is accomplished primarily through three mechanisms, stroking of the seats, stroking of the landing gear and crushing of the fuselage sub-floor structure (Fig. 1.1). Due to cost, complexity and efficiency, the seating system is the optimum location for occupant energy protection.

1.2 Crash Energy Absorption Mechanisms

A crashworthy helicopter seat comprises a seat member including a back section and a seating section and an energy absorbing means connected between the seat member and the frame of the helicopter. These crashworthy seat assemblies have been developed to stroke (i.e. to move usually in a downward direction relative to the aircraft floor) upon severe impact and usually activate energy absorbing devices thereby absorbing all or a portion of the crash energy transmitted to the seat. Energy attenuating seating systems are currently the most effective location for providing occupant energy protection in operational aircraft since the performance of energy attenuating seating systems are less affected by impact attitude and surface than energy attenuating landing gear or sub-floor structure [6]. The most efficient and therefore the most effective process for limiting loads is one that absorbs or dissipates energy rather than one that stores it.

The first Energy Attenuators (EAs) used in crashworthy seating systems stroked at single load value. These were termed Fixed-Load Energy Absorbers (FLESs). These devices are designed to provide a survivable deceleration environment for the 50^{th} percentile occupant weight during pulse [3].

As energy absorbing seat technology was developed for helicopters, many energy absorbing mechanisms or concepts were proposed, developed and fielded in operational systems. All adopted systems are versions of, and/or improvements of, previously considered

concepts [3]. The most common concepts that were suggested, analyzed or tested during the 1960's and 1970's are listed below:

- Crushable Column
- Rolling Torus
- Inversion Tube
- Cutting or Slitting
- Tube and Die
- Rolling/Flattening a Tube
- Strap, Rod, or Wire Bender
- Wire-Through-Platen
- Deformable Links
- Elongation of Tube, Strap, or Cable
- Tube Flaring
- Housed Coiled Cable
- Bar-Through-Die
- Hydraulic
- Pneumatic

The seat analyzed and optimized in this thesis will consist of a Fixed-Load Energy Absorber (FLEA).

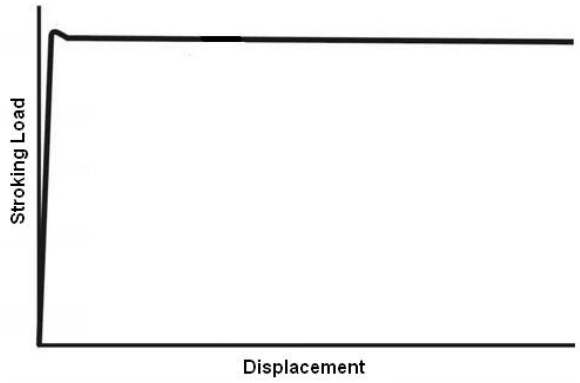

Figure 1.2: Typical Load-deflection curve for a FLEA (Ref 7)

A typical load deflection curve of such an Energy Attenuation system is shown in Figure 1.2. The goal of the crashworthy seat is to absorb and attenuate the kinetic energy of the stroking load as it moves over the stroking distance, thereby transferring the kinetic energy away from the passenger. Because the human spine can only withstand limited compressive forces, inadequate energy absorption by a crashworthy aircraft seat during a hard landing or crash can result in serious spinal injury or death [8]. For typical crashworthy seats, the weight of a seat portion, the passenger, and the passenger's gear combine to create a "stroking load".

There are many factors that affect the weight of passengers or troops in a crashworthy aircraft seat, including: whether the individual is male or female, the troop's weight percentile, and whether the troop is equipped with gear or not. For example it might range from an unequipped female troop in the 5th percentile weighing 110 pounds to a male troop in the 95th weight percentile weighing about 241 pounds.

1.3 Standards Used for Crashworthy Seats

“Design and testing requirements for helicopter crashworthy seats were formulated for both military and civilian aircrafts. In the early seventies, design and test methodologies for military aircraft were developed under the sponsorship of the U.S. Army”. [3] The Aircraft Crash Survival Design Guide, containing criteria for the design of all crashworthiness features, including seats, was first published in 1967 as Technical Report 67-22. Updated revisions were published in 1970, 1971, 1979 and 1989. Detailed requirements for military crew seats were further defined in MIL-S-58095(AV), which was first released in 1971 with the “A” revision being released in 1986. Detailed requirements for military troop seats were defined in MIL-S-85510(AS), which was issued in 1981, and civil rotorcraft seats in SAE, AS8049 which was first issued in 1990 and revised in 1997 [3].

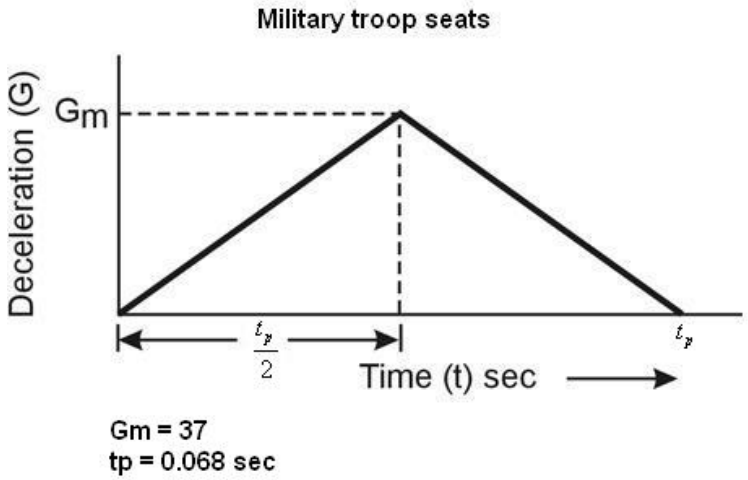

Figure 1.3: Deceleration-time relationship for a military troop seat (Ref 9)

Studies indicated that significant differences exist in the crash environments of military and civilian helicopters. If the military crash resistance design criteria were applied to the civil fleet, a severe weight and cost penalty would be imposed on civilian helicopters. The deceleration-time relationship for military troop seats was used from MIL-S-85510(AS) and is as shown in Figure 1.3.The static and dynamic test requirements for civil and military crashworthy seats are as shown in Table 1.2 [10],

Table 1.2: Static and dynamic test requirements for crashworthy seats (Ref 10)

	Civil		**Military**	
Test requirements of:	JAR/FAR Part 27	JAR/FAR Part 29	MIL-S-58095A(AV)	MIL-S-85510(AS)
Applicable for:	Normal category rotorcraft	Transport category rotorcraft	Cockpit seats	Troop seats
Static tests				
Forward	16	16	35	30
Minimum load factor, G	98 (216)	98 (216)	114 (250)	110 (242.2)
Mass ATD[4], kg (lb)				
Aftward		1.5	12	12
Minimum load factor, G		98 (216)	114 (250)	110 (242.2)
Mass ATD, kg (lb)				
Lateral	8	8	20	20/23[1]
Minimum load factor, G	98 (216)	98 (216)	114 (250)	110 (242.2)
Mass ATD, kg (lb)				
Downward	20	20	25	14.5
Minimum load factor, G	75 (165)	75 (165)	91 (200)	77.5 (170.85)
Mass ATD, kg (lb)				
Upward	4	4	8	8
Minimum load factor, G	98 (216)	98 (216)	114 (250)	110 (242.2)
Mass ATD, kg (lb)				
Dynamic tests				
Test 1 (vertical)				
max. peak deceleration, G			51	37
min. peak deceleration, G	30	30	46	32
time to max. peak, sec			0.043	0.059 (0.034)[2]
time to min. peak, sec	0.031	0.031	0.061	0.087
velocity, m/s (ft/s)	9.14 (30)	9.14 (30)	15.2 (50)	15.2 (50)
roll angle, degrees	0	0	10	10
pitch angle, degrees	60	60	60	60
yaw angle, degrees	0	0	0	0
Mass ATD, kg (lb)	77 (170)	77 (170)	105 (230)	77.5 (170.85)
Percentile	50	50	95	50
limit load factor, G	12	12	0.3048 (12)[3]	14.5
Test 2 (longitudinal)			14.5	
max. peak deceleration, G			33	27
min. peak deceleration, G	18.4	18.4	28	22
time to max. peak, sec			0.066	0.081
time to min. peak, sec	0.071	0.071	0.100	0.127
velocity, m/s (ft/s)	12.8 (42)	12.8 (42)	15.2 (50)	15.2 (50)
roll angle, degrees	0	0	0	0
pitch angle, degrees	0	0	0	0
yaw angle, degrees	10	10	30	30
Mass ATD, kg (lb)	77 (170)	77 (170)	105 (230)	110 (242.2)

Notes:

1. 20 for light fixed-wing, attack, and cargo helicopters.

   23 for utility and observation helicopters.
2. Requirement for research and development testing.
3. According to the Aircraft Crash Survival Design Guide:

   - Cockpit seats: 6 inch minimum.

   - Cabin seats: 12 inch minimum.
4. ATD = Anthropomorphic Dummy

1.4 Objective and Approach

Crashworthy helicopter seats are usually tested in a lab environment using heavy duty equipment to reproduce the crash impact pulse, and the major criteria during the test is to verify whether the seat strokes to the required limit to reduce the deceleration of the occupant. The other major areas of focus are occupant motion and loads on the occupant's critical joints.

The main objective of this research is to carry out structural analysis and optimization of a helicopter crashworthy troop seat assembly using finite element methods. The transient dynamic nonlinear finite element analysis helps in identifying whether the seat structure will survive in a crash landing situation, and optimization helps in reducing the weight of the crashworthy seat. The following steps summarize the research approach,

- To develop a mathematical model of the crashworthy seat using the selected Simula troop seat (type number: PM 1047W-1) and a 50^{th} percentile U.S. army male aviator.
- Application of crash pulse defined for troop seats to the dynamic model in both MATLAB and ANSYS to extract the deceleration profile of the seat.
- To generate a detailed FE model of a crashworthy seat using Pro/Engineer Wildfire 3.0 and ANSYS Workbench v11.0

- To carry out the transient dynamic simulation in ANSYS Workbench using nonlinear elements to represent some of the seat support components and also the energy absorption structure to reduce computation time and also due to limited available computational abilities.
- To optimize selected seat components using Design of Experiments (DOE) methods.

CHAPTER 2

SEAT DYNAMIC MODEL

2.1 Design Parameters

This chapter will describe the dynamic model of the seat, seat occupant and the seat energy absorption system during impact. Equations of motion for this model can be solved to determine the dynamic response of the occupant body, and seat with the crash energy absorption mechanism. The model will be made for a 50th - percentile (170 lb) U.S. Army male aviator which is the size of the anthropomorphic dummy to be used in the actual impact test from military standard MIL-S-85510(AS) [11].

Figure 2.1: Seat-occupant configuration (Ref 12)

The dynamic model for the seat-occupant configuration shown in Figure 2.1 is modeled as a spring-mass system with an input acceleration pulse at the base. The weight of the seat frame is calculated using the model of the seat built in Pro/Engineer Wildfire 3.0 and the weight

of the occupant is selected from available anthropometric data for U.S. Army male aviators. A summary of this anthropometric data is as shown in Table 2.1 [13],

Table 2.1: Weight distribution of U.S. Army male aviators (Ref 13)

	Percentiles		
Measurement	**5th**	**50th**	**95th**
Weight (lb)	133	170	212

The nonlinear spring in the model represents the energy attenuation (EA) absorption mechanism. This could be a crushable column, rolling torus, inversion tube, tube and die or a metal cutter type energy absorber. In this research, a composite (Gr/Ep) tube energy absorber is used for analysis. The Gr/Ep tube attenuates forces generated upon high velocity impact, such as in crash situations. Under high impact landing conditions, energy is dissipated through the permanent deformation, or crushing, of the energy absorber as shown in Figure 2.2 [14].

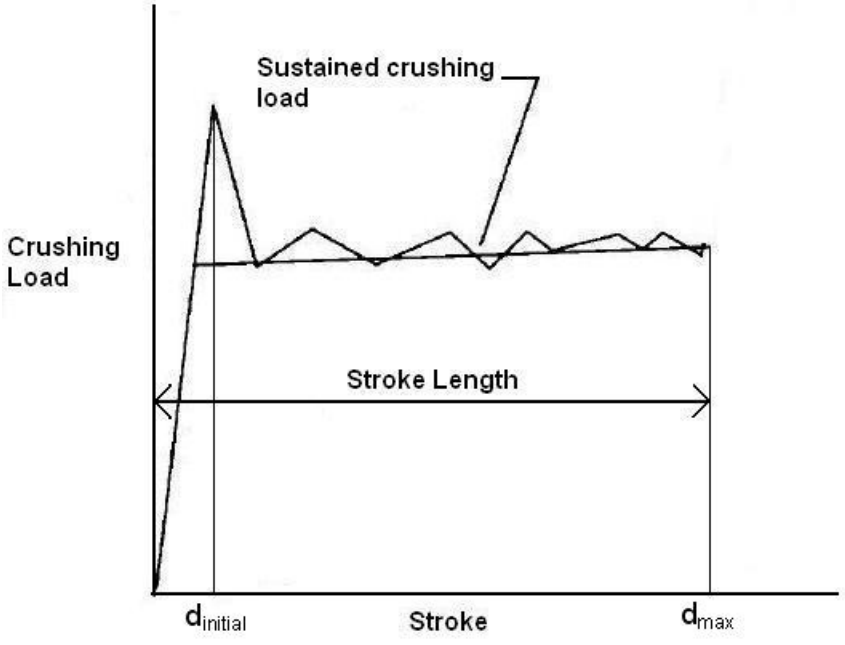

Figure 2.2: Typical load-stroke length showing stroke length (Ref 14)

Ideal crushing behavior for energy absorption is shown in Figure 2.3. Ideally, load will rise as the tube is crushed to a steady-state level where energy absorption remains constant as the tube is crushed further. In practice, however, crush behavior often deviates from the ideal as shown in Figure 2.3.

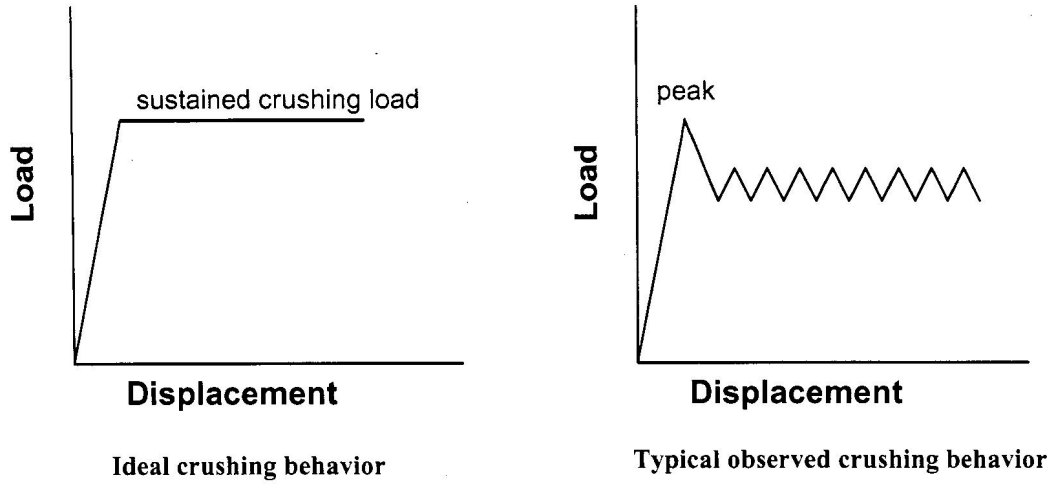

Figure 2.3: Typical and ideal crushing behavior (Ref 15)

In this case, the load will rise to a peak value, but then lower and oscillate around an average steady-state value (Figure 2.3). The difference between peak load and sustained load is called load ratio and should be as small as possible to produce the smoothest deceleration [15]. Due to its complexity, the crushing of the composite tube itself is time & computationally intensive. So the aim in this research is not to model the crushing behavior of the composite tube, but to try and duplicate its behavior taken from an existing test to find out its effects on the structure of the selected crashworthy seat. Also the peak load of the tube can be designed to be higher or lower depending on the weight of the seat-mass configuration by adjusting the cone angle or changing the thickness of the tube.

A typical load-deflection curve for a graphite/epoxy crash tube is shown in Figure 2.4 [16].

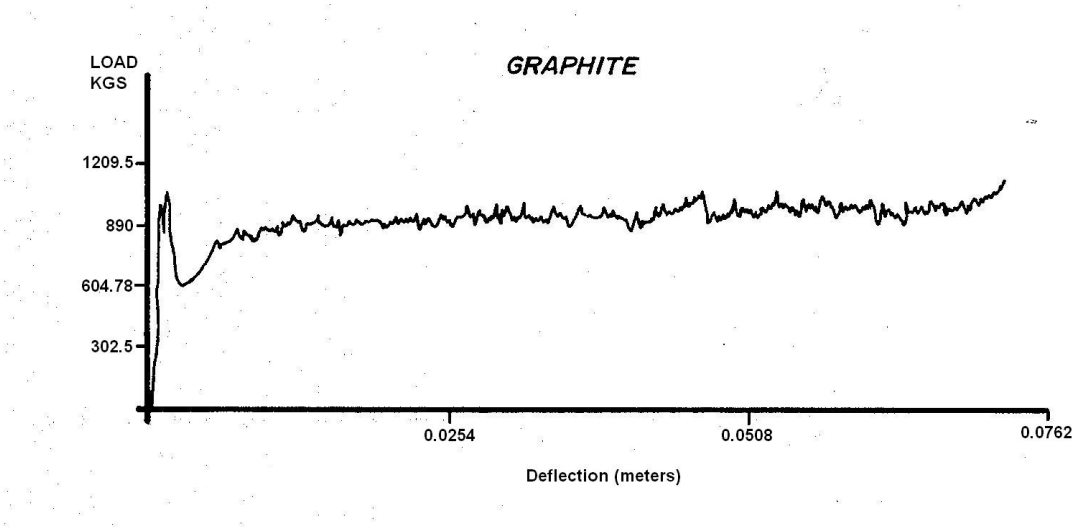

Figure 2.4: Load vs deflection for a Gr/Ep tube (Ref 16)

The response of the Gr/Ep tube EA is converted into an ideal response and divided into two regions with linear responses. Region I has a slope k1 with a cutoff load of 907.18kg and region II maintains the constant load of 907.18 kg throughout the length of the stroke of the EA. This load-deflection curve is shown in Figure 2.5,

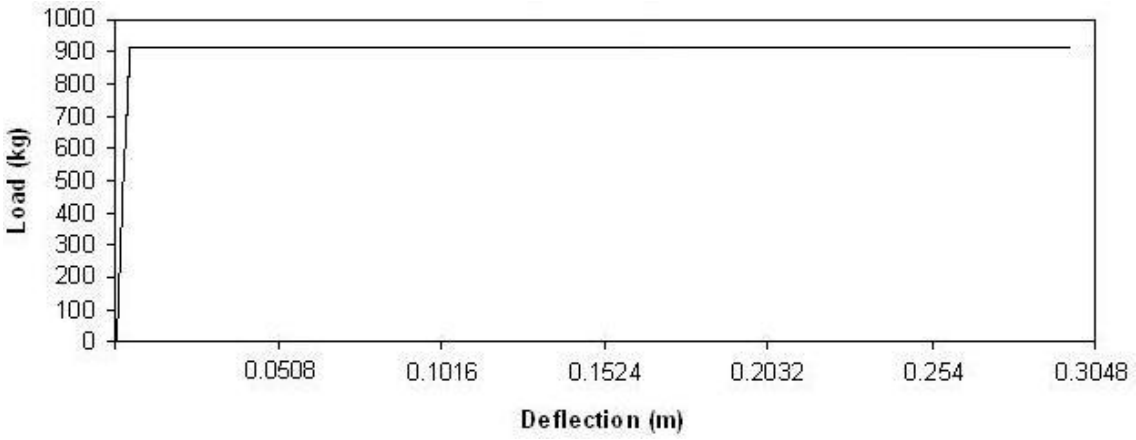

Figure 2.5: Ideal load-deflection curve

This research deals only with energy absorption in the vertical (Z axis relative to the seat and occupant) crash load direction and the systems developed to attenuate, or limit, the resulting loads on occupants of military helicopters. A triangular impact acceleration pulse is applied to the aircraft sub-floor represented by a fixed support. This acceleration pulse has a peak load of 37 G's and reaches its peak in 0.034 sec. The complete pulse is over a period of 0.068 sec. The deceleration-time relationship (pulse) developed for the design of this system is taken from military standard, MIL-S-85510(AS) [9] (Figure 2.6).

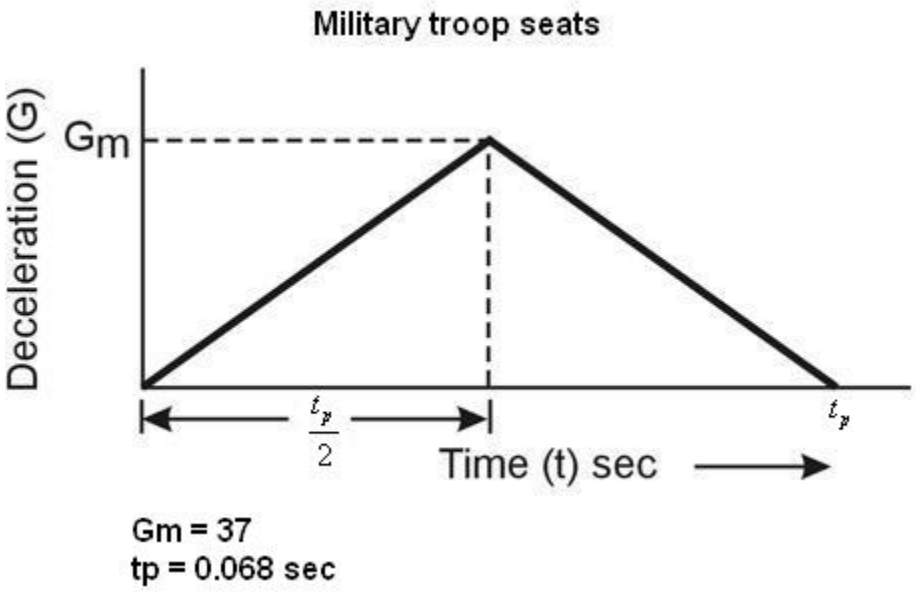

Figure 2.6: Deceleration-time pulse for Military troop seats (Ref 9)

2.2 Mathematical Model

As mentioned in the previous section, a single degree of freedom lumped mass system (Figure 10) represents the seat and the energy attenuation system and the triangular pulse shown in Figure 2.7 is applied to the aircraft floor (fixed support).

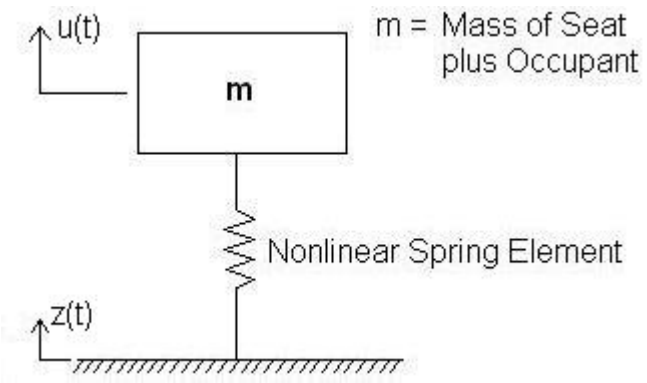

Figure 2.7: SDOF system responding with motion *u*(t) to base motion *z*(t)

where,

z(t) = Displacement of base and

u(t) = Displacement of mass

The triangular pulse can be described by its amplitude of acceleration G_m and its duration t_P as shown in Figure 2.6. The forcing function can be divided into three regions, and the pulse-time history is expressed as,

$$f(t) = \frac{2G_m}{t_p} * t \qquad 0 \le t \le \frac{t_p}{2} \qquad \text{(Eq. 2.1)}$$

$$f(t) = 2G_m\left(1 - \frac{t}{t_p}\right) \qquad \frac{t_p}{t} < t < t_p \qquad \text{(Eq. 2.2)}$$

$$f(t) = 0 \qquad t \ge t_p \qquad \text{(Eq. 2.3)}$$

The free body diagram for above system has a spring force and an inertia force acting in the direction shown in Figure 2.8,

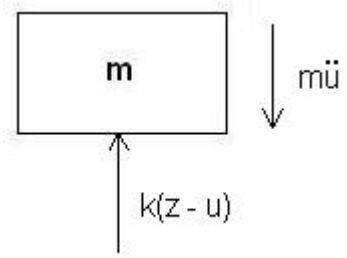

Figure 2.8: Free body diagram

The general equation of motion can be found over two stages as follows,

First Stage ($0 < t < \frac{t_p}{2}$):-

$$-m\ddot{u} + k(z-u) = \frac{2G_m t}{t_p} \qquad \text{(Eq. 2.3)}$$

Second Stage ($\frac{t_p}{2} < t < t_p$):-

The impact load during the second stage can be considered as the sum of a constant acceleration with amplitude $2G_m$ and a negative ramp load given by $-2G_m \frac{t}{t_p}$. The load-induced response can then be obtained by superimposing the responses due to both loads.

$$-m\ddot{u} + k(z-u) = 2G_m\left(1 - \frac{t}{t_p}\right) \qquad \text{(Eq. 2.4)}$$

2.3 MATLAB and ANSYS Simulations

The equations derived in the previous section are solved using MATLAB and the SDOF system is also simulated in ANSYS. The seat is assumed to be at rest initially, and then an acceleration impact pulse is applied to the aircraft sub-floor (fixed surface in model).

2.3.1 MATLAB Simulation

The ordinary differential equations representing the system are solved using the 4th order Runge-Kutta method (Appendix A.1). The inbuilt MATLAB function called ODE45 which uses the Runge-Kutta method is used for this purpose.

The constants used are [9], [16],

Gm = Peak acceleration = 362.97 m/s^2

tp = Pulse duration = 0.068 sec

m = Mass of seat and occupant = 83 kg

Solution time steps are,

minstep = 1.00E-15

maxstep = 0.0005

The nonlinear spring is divided into two regions with properties,

k1 = Initial slope = (8902.39 N / 0.000762 m) = 11682933.7 N/m

k_cutoff = Cutoff displacement = 0.000762 m

k2 = 8902.39 N

The results of the above simulation are shown in Figures 2.9, 2.10 and 2.11,

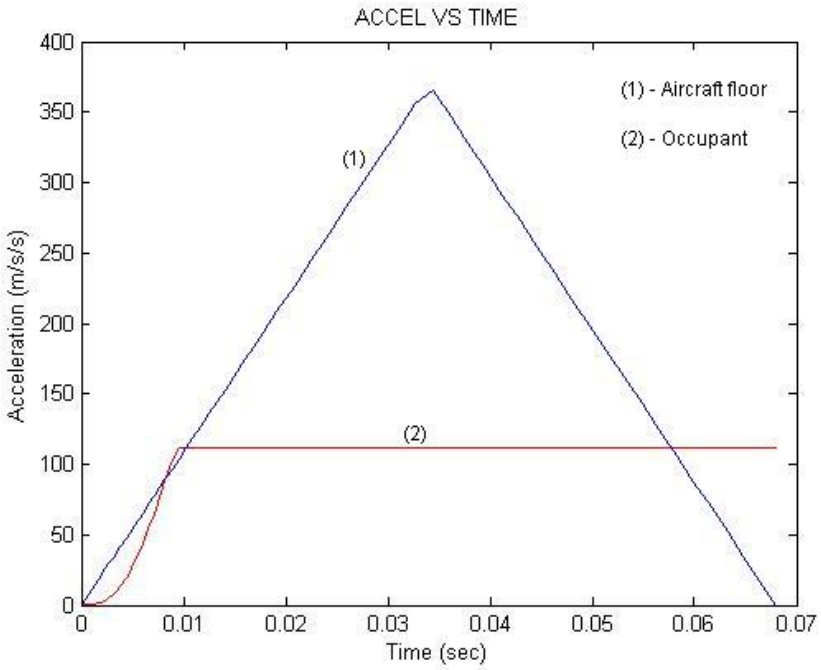

Figure 2.9: MATLAB Results – Acceleration vs Time

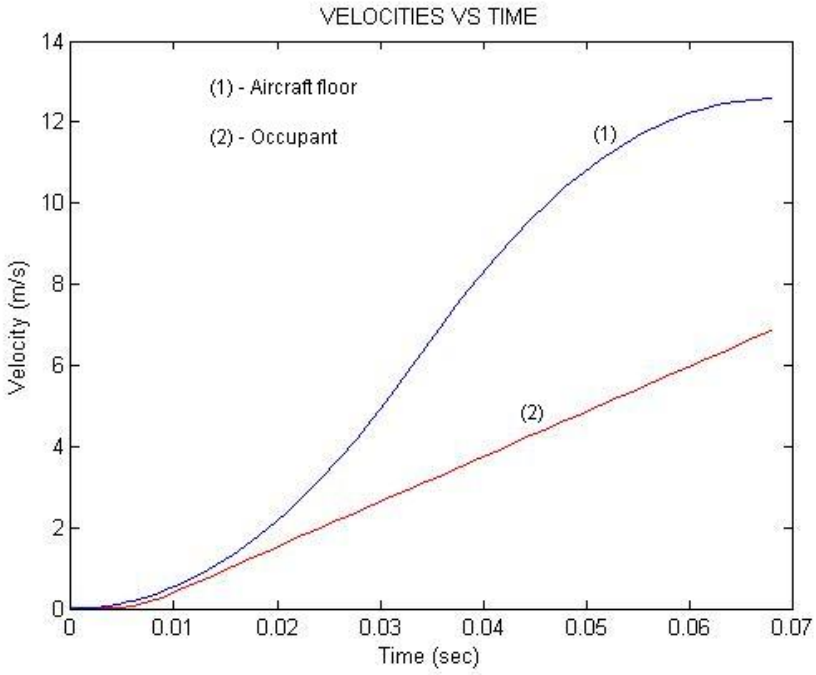

Figure 2.10: MATLAB Results – Velocity vs Time

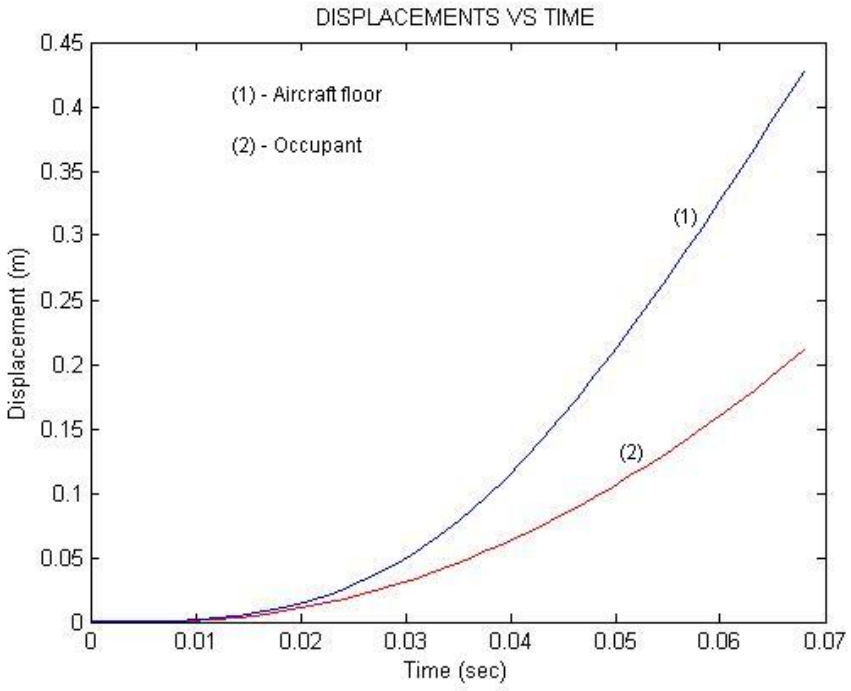

Figure 2.11: MATLAB Results – Displacement vs Time

The acceleration vs time graph (Figure 2.9) shows that the deceleration of the occupant is limited to 13.125 G's which is below the specified limit of 14.5 G's from MIL-S-85510(AS) thus eliminating the chances of damage to the spinal cord.

The displacement vs time graph in Figure 2.11 shows the displacement of the occupant and the aircraft sub-floor in a crash landing situation. The relative displacement between the two indicates that the stroke of the energy attenuating mechanism is 0.2 m (0.4125 m – 0.2125 m). In other words the occupant will travel a distance of 0.2 m towards the aircraft sub-floor and this should be taken into consideration while manufacturing the seat support systems.

2.3.2 ANSYS Simulation

A nonlinear simulation is carried out in ANSYS using the same SDOF spring-mass system (Appendix B.1). The Mass21 element was used to represent the mass of the seat and occupant while COMBIN39 element was used to represent the nonlinear spring.

The constants used are,

Max_G = Peak acceleration = 362.97 m/s^2

Pulse_t = Pulse duration = 0.068 sec

m = Mass of seat and occupant = 83 kg

The real constants defined for COMBIN39 element includes the definition of a force-deflection curve along with setting some KEYOPTS which define the behavior of the spring. The force-deflection curve is defined in Table 2.2,

Table 2.2: Force vs deflection values

Deflection (m)	Force (N)
0.000762	8899.48
0.254	8899.48

The KEYOPTS are set such that the spring element is a 2D element; unloads along same path; compressive loading follows defined compressive curve and displacement is along nodal X axis. The resulting displacement vs time graph is shown in Figure 2.12 below,

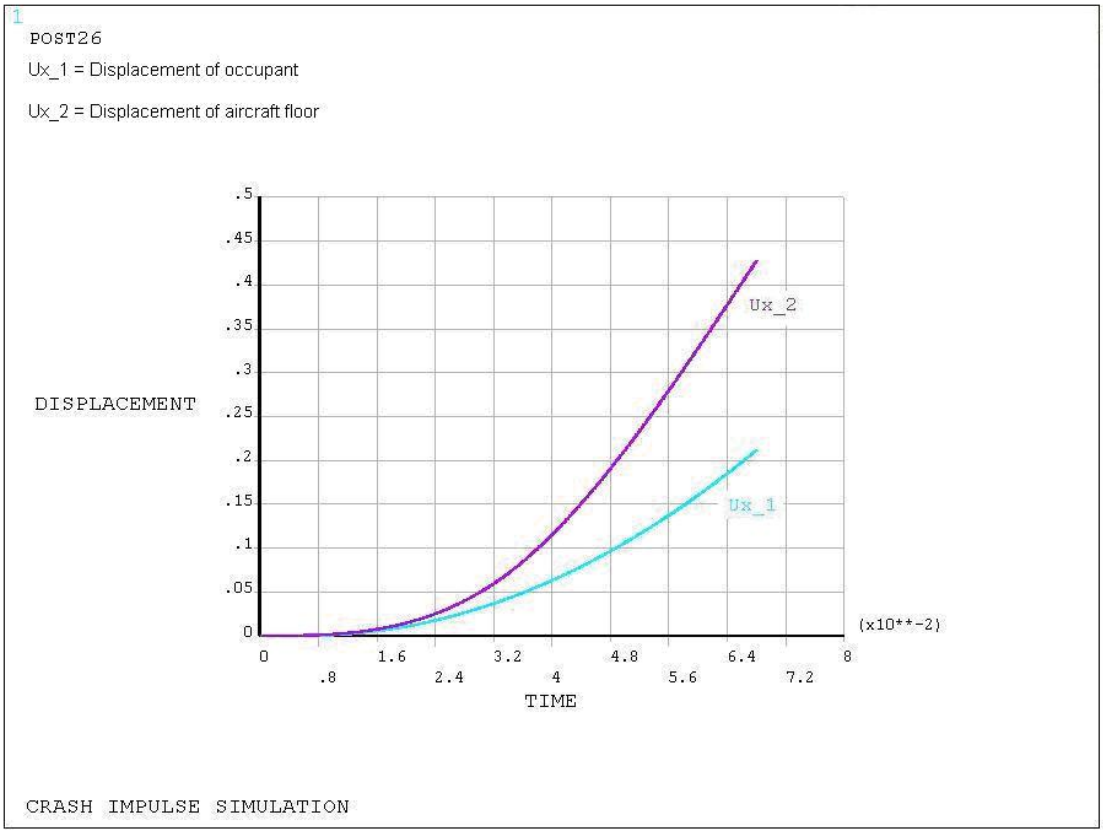

Figure 2.12: ANSYS Result – Displacement vs Time

Thus from the above displacement vs time plot we can see that the stroke of the energy attenuating mechanism is 0.1975 m (0.4125 m – 0.215 m) which matches closely with the results from the MATLAB simulation (0.2 m) thus validating the dynamic model, and therefore we can use the calculated deceleration profile of the occupant for the crash simulation of the complete seat assembly.

CHAPTER 3

IMPACT SIMULATION IN ANSYS

3.1 Seat Characteristics

The basic requirements of crash survival are to maintain a livable volume, restrain the occupant, prevent the structure of the seat from failing, keep occupant crash loads within human non-injury tolerance and provide means and time to escape. We will concentrate on the structure of the seat to check whether it is safe in a crash situation.

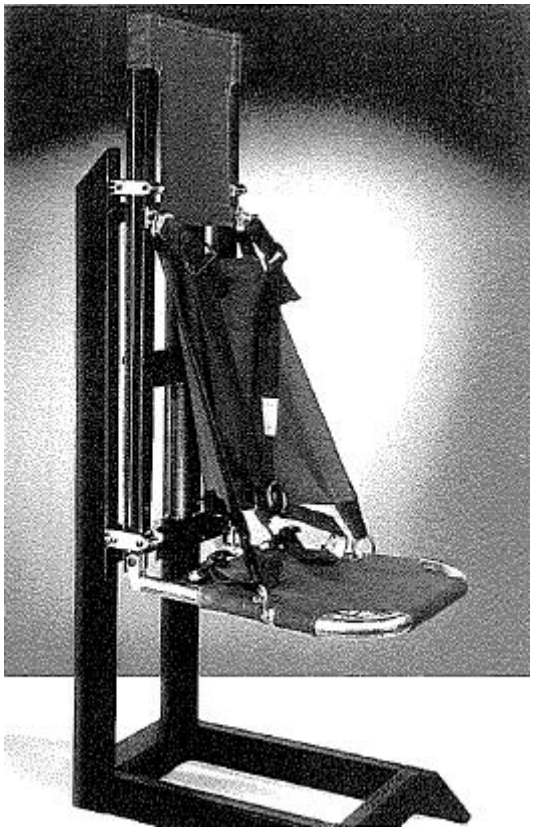

Figure 3.1: Image of the troop seat (Ref 10)

The layout of the seat used for this analysis is based on an existing Simula troop seat (type number: PM 1047W-1) [10]. The backside of the seat system is manufactured of C/Ep with stacking sequence $[+45/-45]_{2S}$. This backside is made of an H-shaped frame which moves vertically in one piece with the seat itself. The profiles used as vertical members are two I-shaped profiles, while the cross connection is formed by one U-shaped profile. The energy absorbing crash system is situated between this U-shaped profile and a second U-shaped profile which is connected between two fixed fuselage/cabin frame connection points [10]. The overall dimensions in mm of the seat are shown in Figure 3.2.

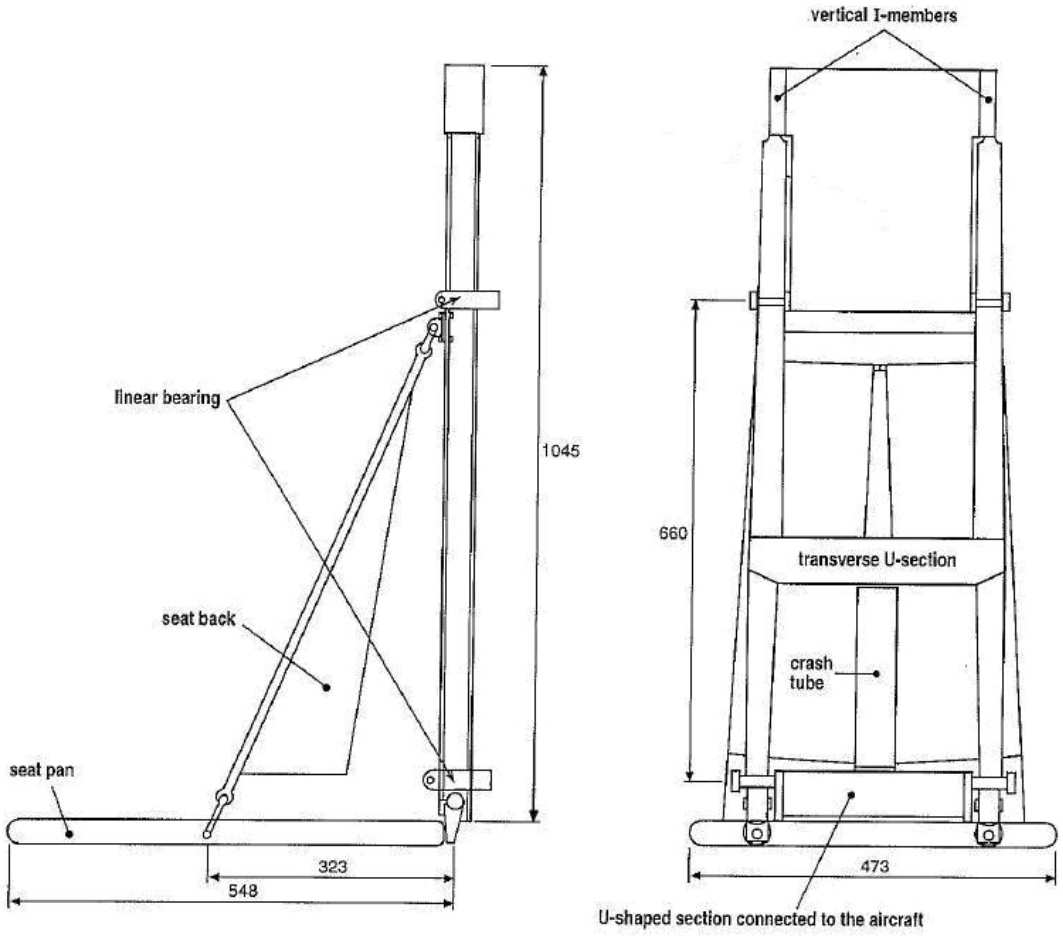

Figure 3.2: Overall dimensions in mm of troop seat (Ref 10)

Pro/Engineer Wildfire 3.0 was selected for building the parametric CAD model because of the compatibility between the ANSYS Workbench and Pro/E modules. The Pro/Engineer Wildfire 3.0 solid model was built using the dimensions provided in Figure 3.2 above. Some assumptions were made while building the CAD model since all the necessary dimensions were not provided in the reference. The seat assembly consists of a total of 13 parts. Figure 3.3 shows the model in Pro/Engineer,

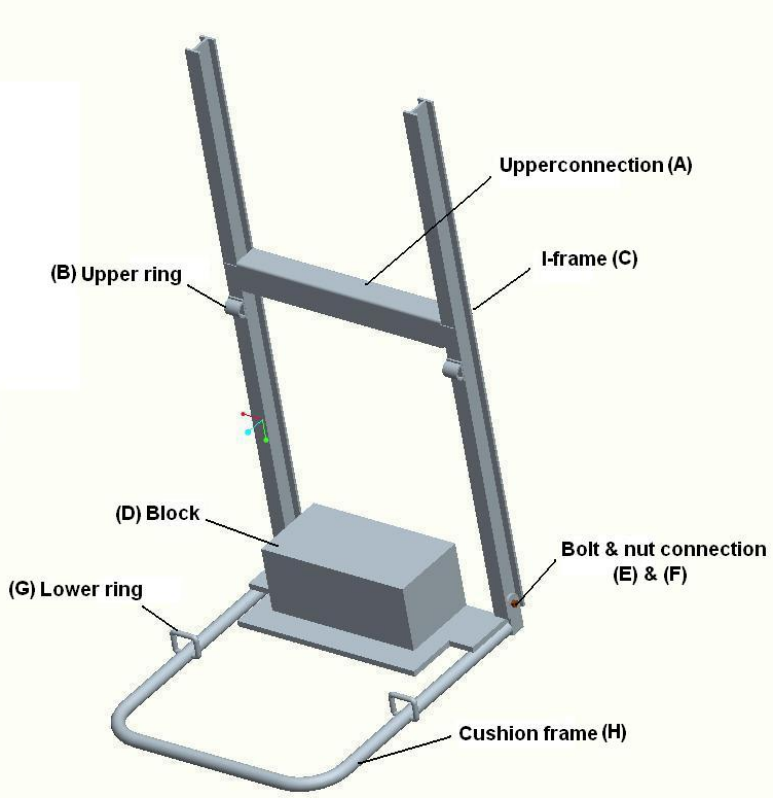

Figure 3.3: Parametric model of seat assembly

An exploded view of above assembly is shown in Figure 3.4,

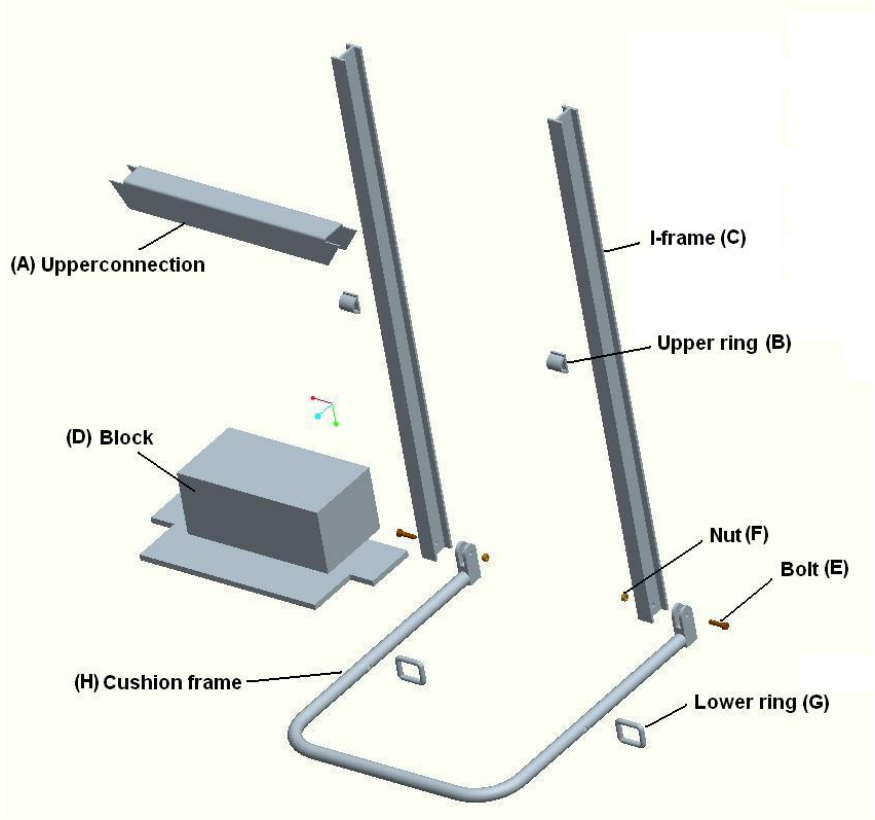

Figure 3.4: Exploded view of assembly

The material properties for the seat components are as shown in Table 3.1 below,

Table 3.1: Material Properties

	Aluminium Alloy	Block material	Steel
Young's Modulus (Pa)	7.5e10	2e11	2e11
Poisson's Ratio	0.33	0.3	0.3
Density (kg/m^3)	2697.7	21486	7850

This seat along with its parameters is then exported in ANSYS Workbench v11.0, and the co-ordinate system is as shown in Figure 3.5,

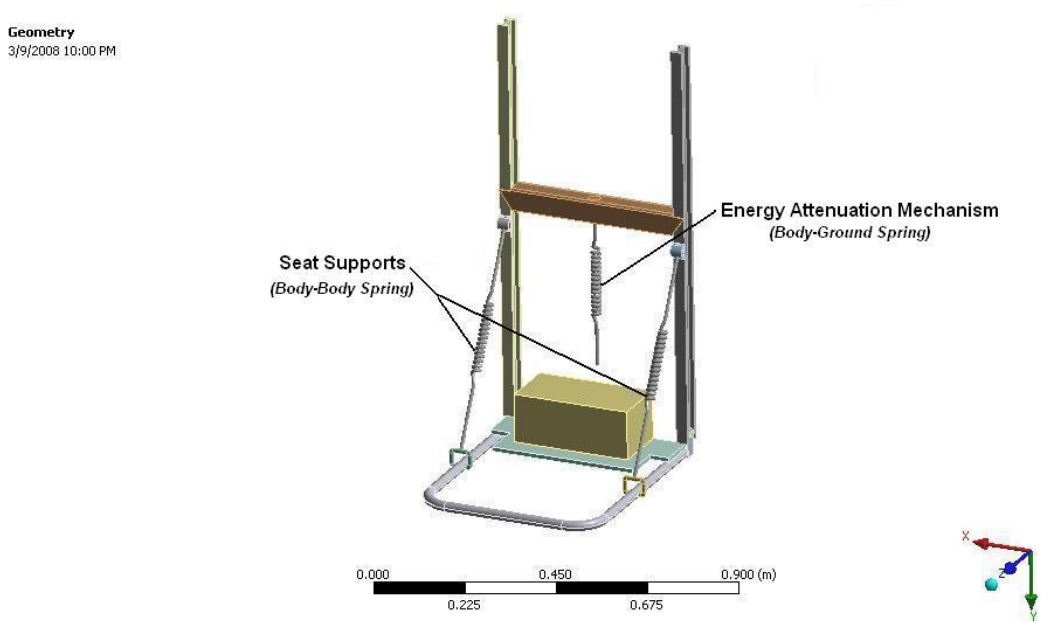

Figure 3.5: Co-ordinate system and nonlinear spring elements

The backside of the seat system is manufactured of C/Ep. This backside is made of an I-shaped frame which moves vertically in one piece with the seat itself. The laminate layup is assumed to be $[+45/-45]_{2S}$, and Lamination theory is used to find the equivalent orthotropic material properties for the C/Ep laminate in the XYZ co-ordinate system shown in Figure 3.5 (Appendix A.2). Since Lamination theory is applicable to a 2D component, reasonable assumptions were made for properties in the third dimension. The orthotropic material properties used for this part are,

Young's Modulus X direction, E_X = 1.039e10 Pa

Young's Modulus Y direction, E_Y = 2.391e10 Pa

Young's Modulus Z direction, E_Z = 2.391e10 Pa

Poisson's Ratio XY = 0.27

Poisson's Ratio YZ = 0.7078

Poisson's Ratio XZ = 0.27

Shear Modulus XY = 7e9 Pa

Shear Modulus YZ = 3.819e10 Pa

Shear Modulus XZ = 3.7e9 Pa

Density = 1600 kg/m^3

The following table provides information about the material properties used for each part,

Table 3.2: Materials Used

Part	**Material**
Cushion Frame	Aluminium Alloy
Upper Ring	Aluminium Alloy
Lower Ring	Aluminium Alloy
Bolt	Steel
Nut	Steel
Upper Connection	Steel
Mass Block	Steel
I-Frame	C/Ep

The bolt used in this application is a 5/16"-18 Grade 8 bolt which is 1.25" long, and the nut is a 5/16"-18 bolt. A table of recommended bolt preload values is used to select the value of preload for the bolts used in the seat assembly. The table is based on the following assumptions [17],

1. The fasteners are commercial grade and made of steel.

2. The nut factor (K) is 0.2, i.e., the fasteners are used in as-received condition and are neither cleaned nor lubricated.

3. The fasteners will be tightened by applying torque to the nut, not to the head.

4. The fasteners are tightened to an average stress (in the threaded section) of 25,000 psi.

Based on the assumptions mentioned above we get a bolt preload value of 1310 lbf from the table for recommended bolt preload values [17].

Table 3.3: Recommended preload value (Ref 17)

Size	Series	Tensile Stress Area As (in^2)	Preload (Fp) at 25 ksi (kip)
5/16-18	UNC	0.0524	1.310

The default spring available for use in ANSYS Workbench 11.0 is a linear spring, but this spring can be converted into a nonlinear spring by inserting a command snippet under the linear spring tab. As mentioned in the previous chapter, a nonlinear spring represents the crash energy absorbing mechanism (Figure 3.5) and is created using APDL commands (Appendix B.2)

This body-ground spring element is scoped to a surface which represents the dimensions of the crash-tube by imprinting a surface on the upper connection (Figure 3.3 (A)) of the seat while the other end is fixed to the ground. The scoped surface is shown in Figure 3.6,

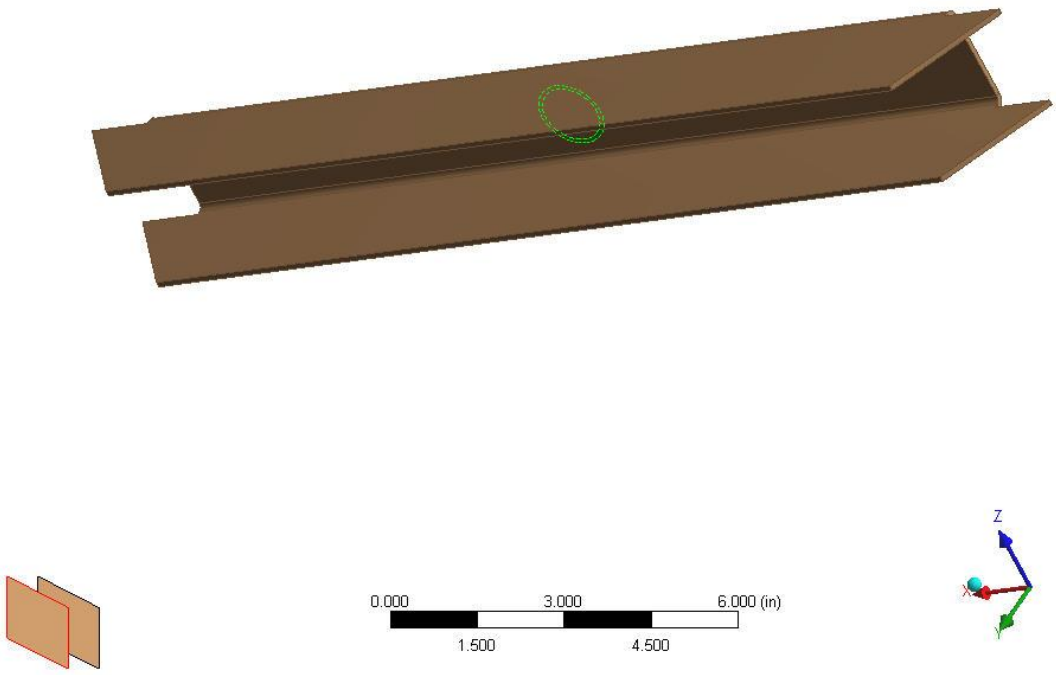

Figure 3.6: Scoped surface on Upperconnection

Two seat supports are provided in the assembly, and are assumed to be made of the kind of materials used for seat belts. The stiffness characteristics of these supports are modeled using nonlinear COMBIN39 elements and the following load deflection curve is used to model their behavior [18],

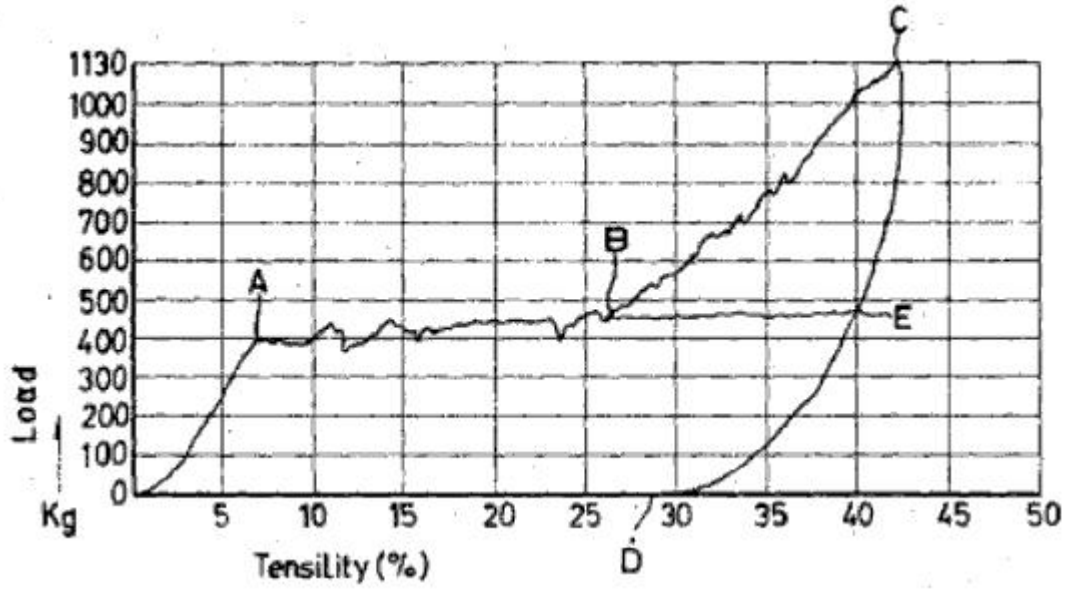

Figure 3.7: Curve indicating the relation between the load and tensility of the seat belt [Ref 18]

A body to body (Body-Body) spring is used for this purpose and the spring behavior is split into three regions with three different slopes as shown in Figure 3.8.

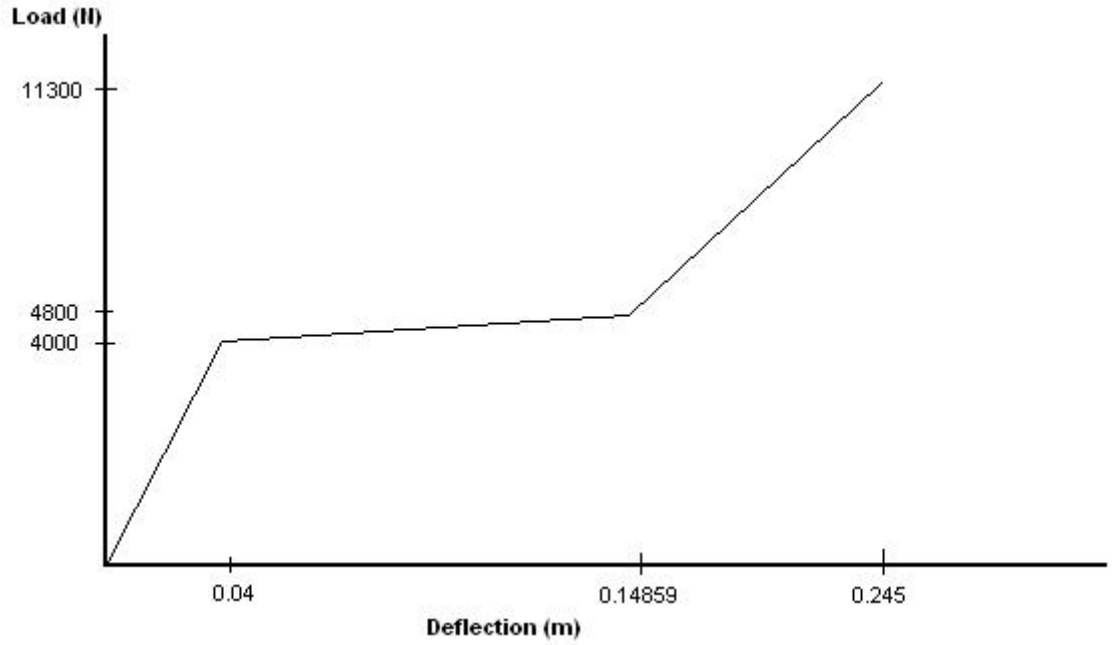

Figure 3.8: Load deflection curve of seat belt

APDL commands are used to create the nonlinear spring and the load-deflection curve in ANSYS (Appendix B.2). These springs are scoped to two surfaces shown in Figure 3.9.

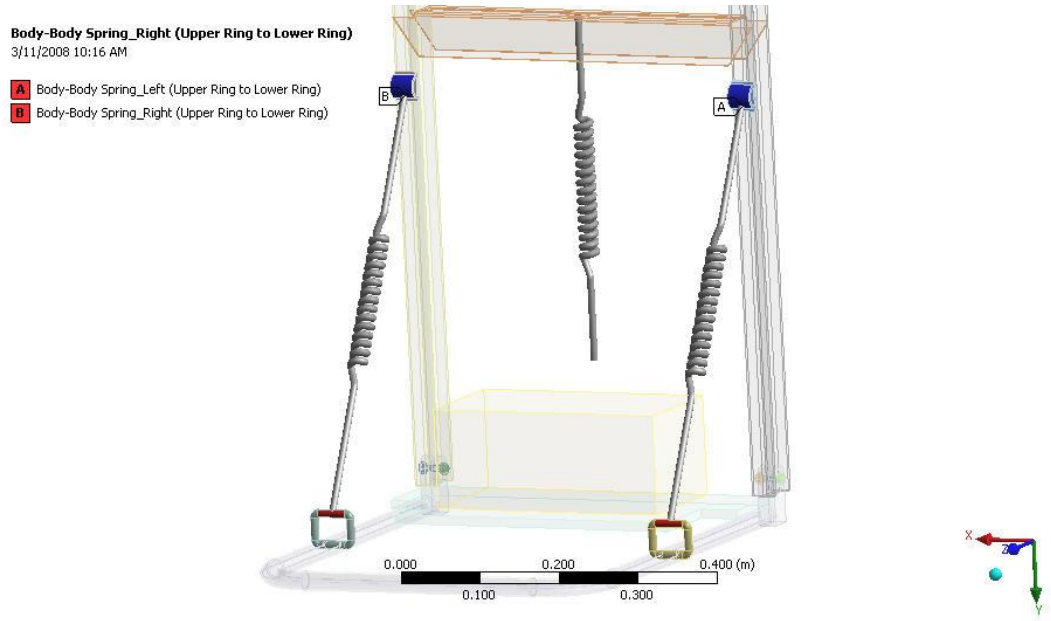

Figure 3.9: Scoped surfaces on Upper and Lower Rings

3.2 Model Setup and Analysis Approach

This analysis was carried out to investigate the structural behavior of the troop seat in a crash landing situation. The setup of the seat is similar to the experimental setup shown in Figure 3.10 with the difference in the use of a mass block instead of the actual anthropometric dummy.

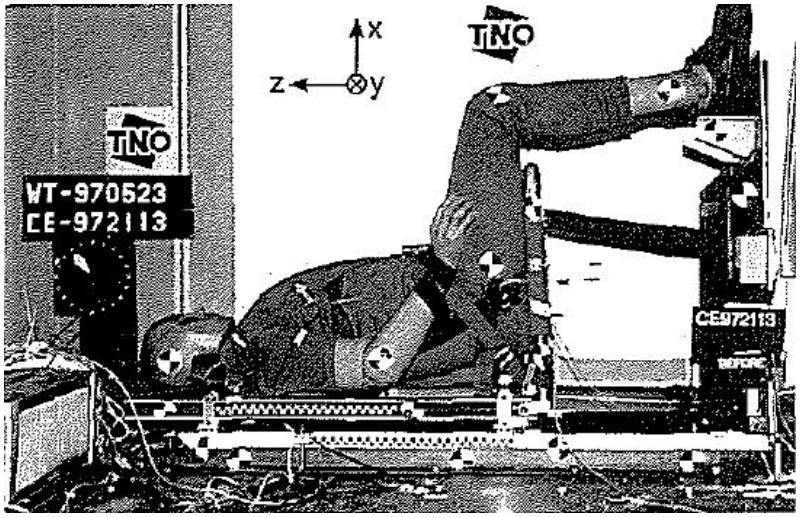

Figure 3.10: Experimental set-up (Ref 10)

To carry out this transient dynamic analysis, the Flexible Dynamic module of ANSYS Workbench is used. Flexible dynamic analysis (also called time-history analysis) is a technique used to determine the dynamic response of a structure under the action of any general time-dependent loads. This type of analysis can be used to determine the time-varying displacements, strains, stresses, and forces in a structure as it responds to any combination of static, transient, and harmonic loads. The time scale of the loading is such that the inertia or damping effects are considered to be important [19].

After the parametric CAD model is imported into ANSYS Workbench from Pro/Engineer Wildfire 3.0, the model is sent into the simulation environment where contact surfaces between the different parts of the seat assembly are automatically detected. Care should be taken while exporting parameters to ANSYS Workbench. This is because if the parameters are not tagged with an extension recognizable by ANSYS, then they will not be exported. The parameters were tagged with the default tag of DS for this model. All the contacts are assumed to be bonded in the assembly. Three nonlinear spring elements are added to the model to represent the crash tube, and the two seat supports as mentioned in the previous section.

The boundary conditions applied to replicate the actual test conditions are:-

1) Vertical I-frame is restricted to move in the Z and the X directions (Figure 3.5) since this I-frame is fitted into roller bearings attached to the aircraft body.

2) Mass block is restricted to move in the X direction to cancel out spurious deflections.

A summary of the loads and boundary conditions is shown in Figures 3.11 and 3.12,

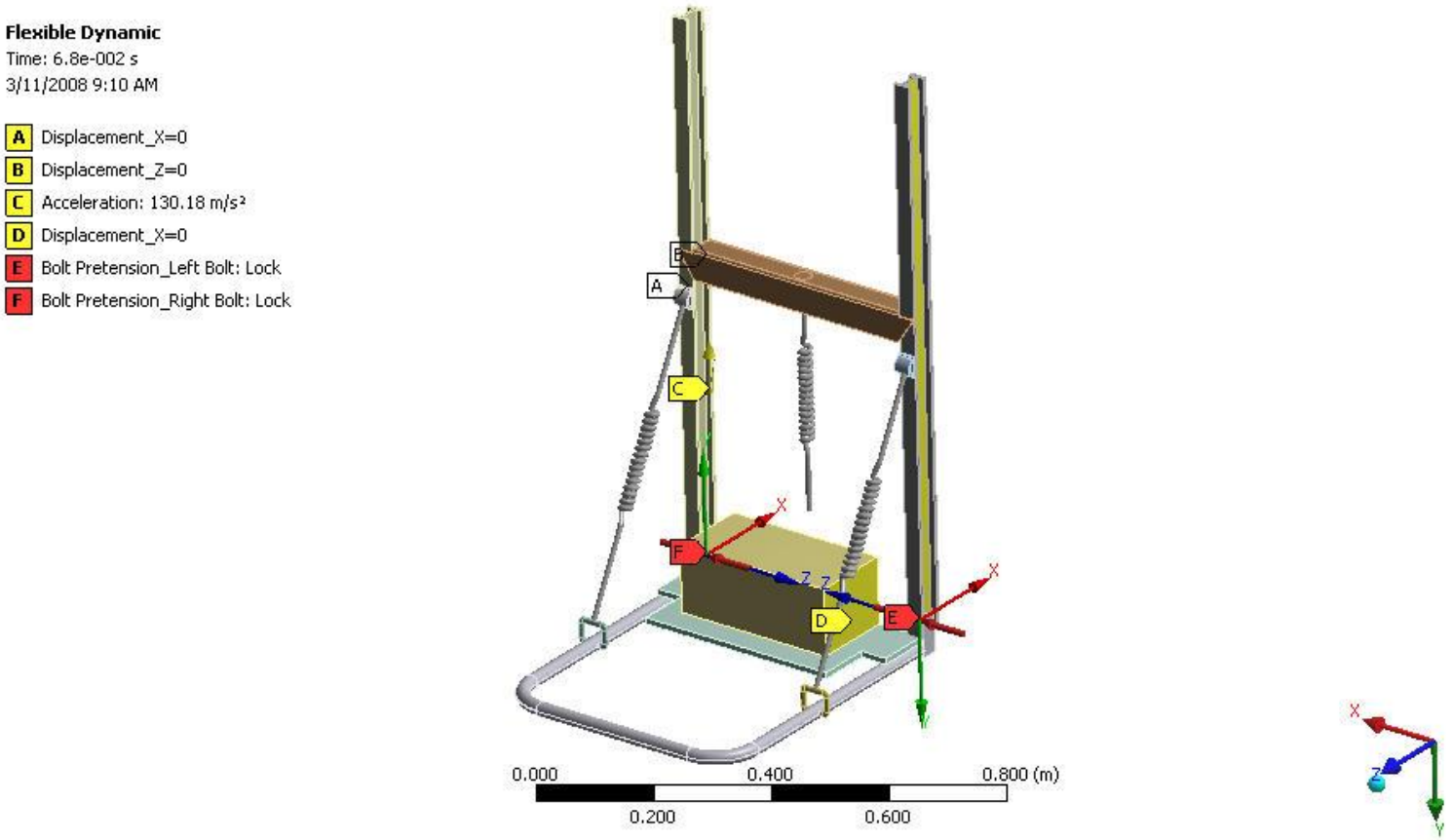

Figure 3.11: Loads and boundary conditions (front view)

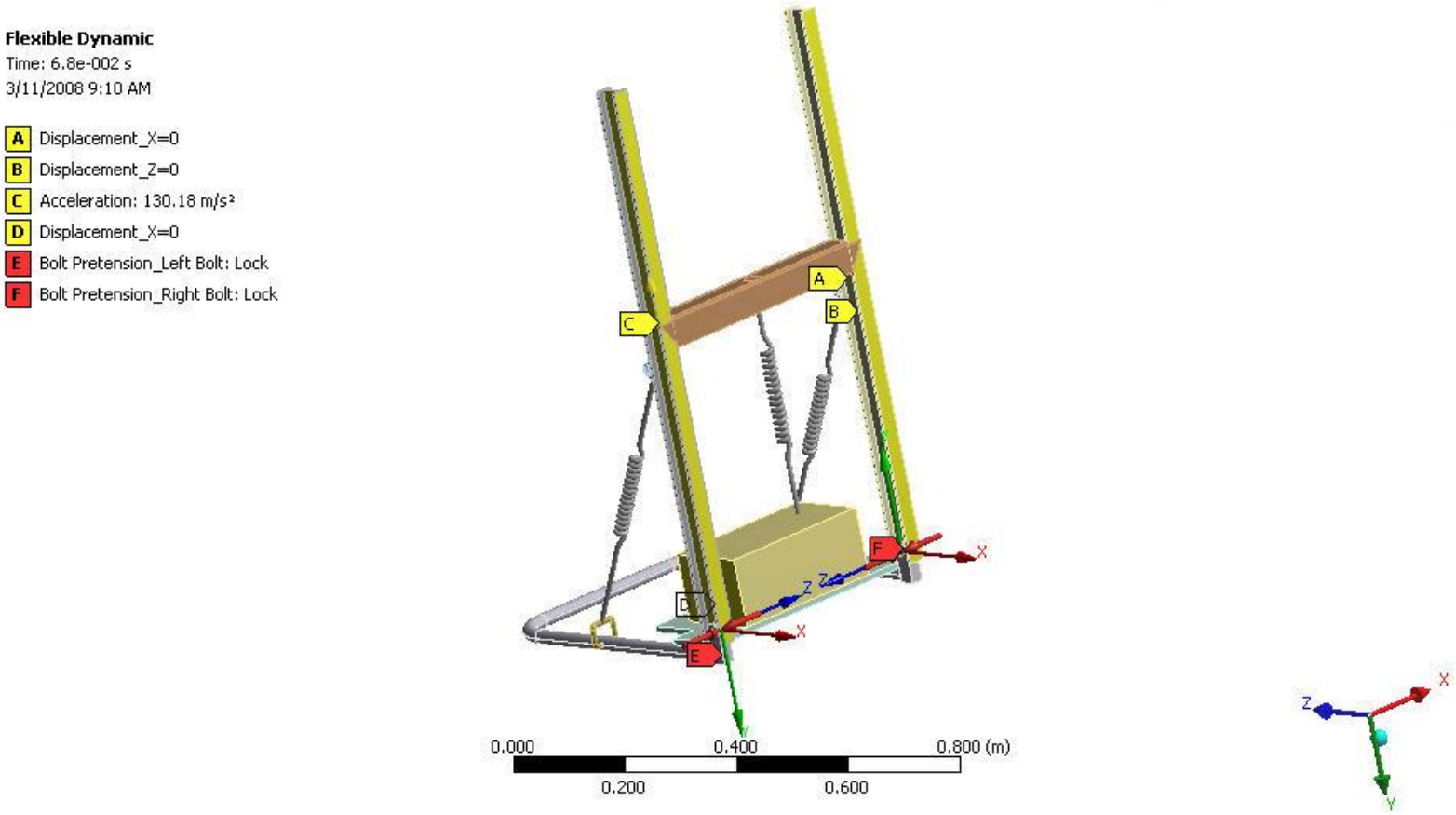

Figure 3.12: Loads and boundary conditions (back view)

An acceleration vs time input (Figure 3.13) is provided to the seat for the transient analysis. This profile is extracted from the SDOF spring-mass MATLAB and ANSYS simulations, and is applied to the seat in ANSYS WB as shown in Figure 3.11.

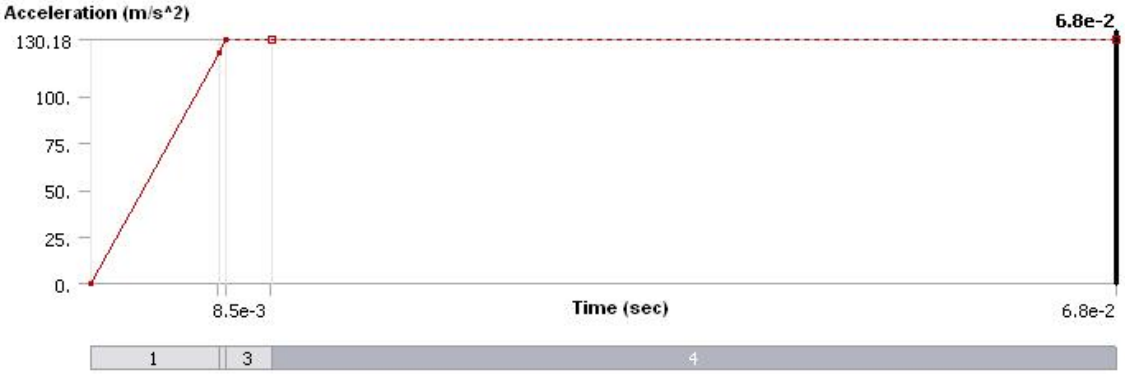

Figure 3.13: Acceleration vs time input

Flexible dynamic analysis settings need to be set before simulating the model. Step Controls were used to control the time step size in a transient analysis. For this case an initial simulation with two steps was carried out, and this provided information about where the change in slope occurs for the spring element during the simulation by following the force-convergence criterion. Using the information obtained, the number of steps was increased to 4 and was strategically placed so that the simulation time is reduced. This was achieved by providing very small step sizes in the region where a change of slope occurs while the rest of the profile had comparatively larger step sizes. The minimum step sizes used for the analysis are 10 µsec for regions 2 and 3, and it is 100 µsec for regions 1 and 4. The step sizes used are shown in Table 3.4.

Table 3.4: Step size settings

	Step 1 0s – 0.0085s	Step 2 0.0085s – 0.009s	Step 3 0.009s – 0.011s	Step 4 0.011s – 0.068s
Initial Time Step (sec)	0.002	0.0001	0.0001	0.002
Minimum Time Step (sec)	0.001	0.0001	0.0001	0.001
Maximum Time Step (sec)	0.01	0.0001	0.0001	0.01

Initially the seat is kept at rest and large deflection is turned on. The mesh of the complete assembly consists of a total of 41,877 elements with 55,129 nodes. A breakup of the type of elements used is shown in Table 3.5.

Table 3.5: Breakup of number of elements

Element Type	Number of Elements
3-D 20-Node Structural Solid (SOLID186)	694
3-D 10-Node Tetrahedral Structural Solid (SOLID187)	23697
3-D 8-Node Surface-to-Surface Contact (CONTA174)	8854
3-D Target Segment (TARGE170)	8555
Nonlinear Spring (COMBIN39)	3
Pretension (PRETS179)	74

After the initial run, the mesh size was refined using h-type refinement in regions under high stresses to get a smooth stress distribution. This was achieved using the sphere of influence feature. A total of seven spheres with desired diameters and centers were defined, and also the size of elements was adjusted accordingly to get the required mesh. Figure 3.14 shows the spheres created in the model for mesh refinement.

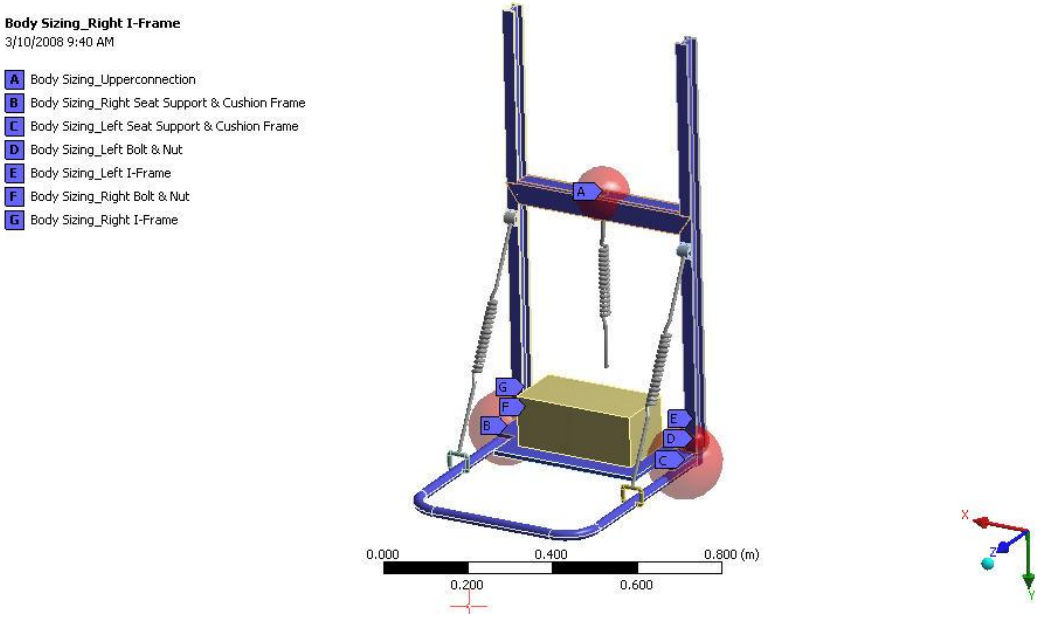

Figure 3.14: Mesh refinement using spheres of influence

The refined mesh is shown in Figures 3.15 and 3.16

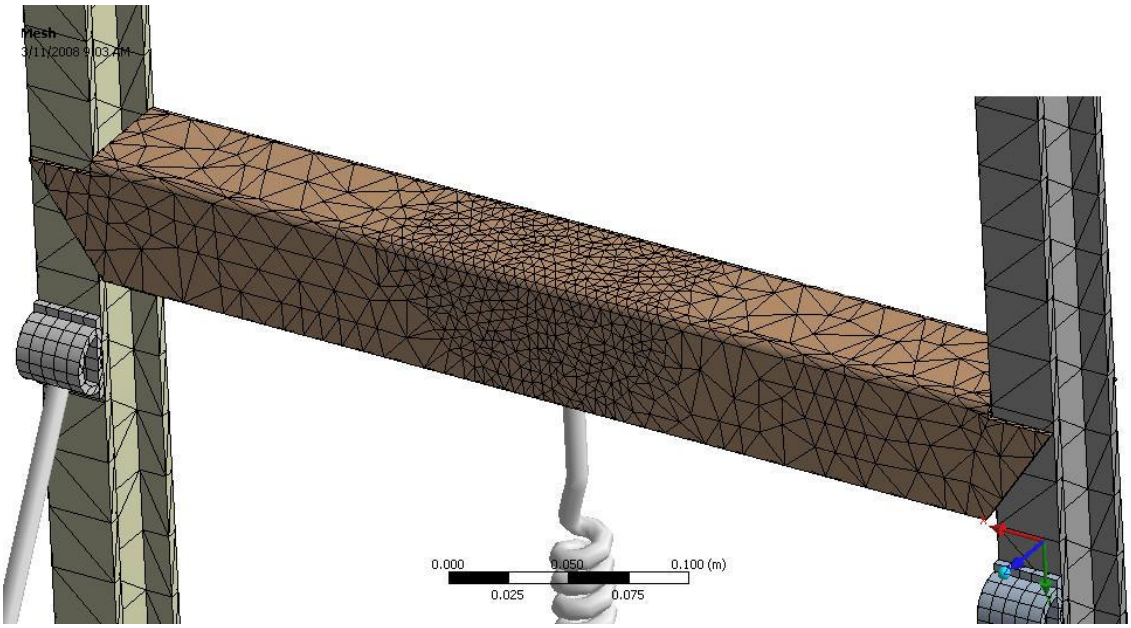

Figure 3.15: Refined mesh in upper section of seat

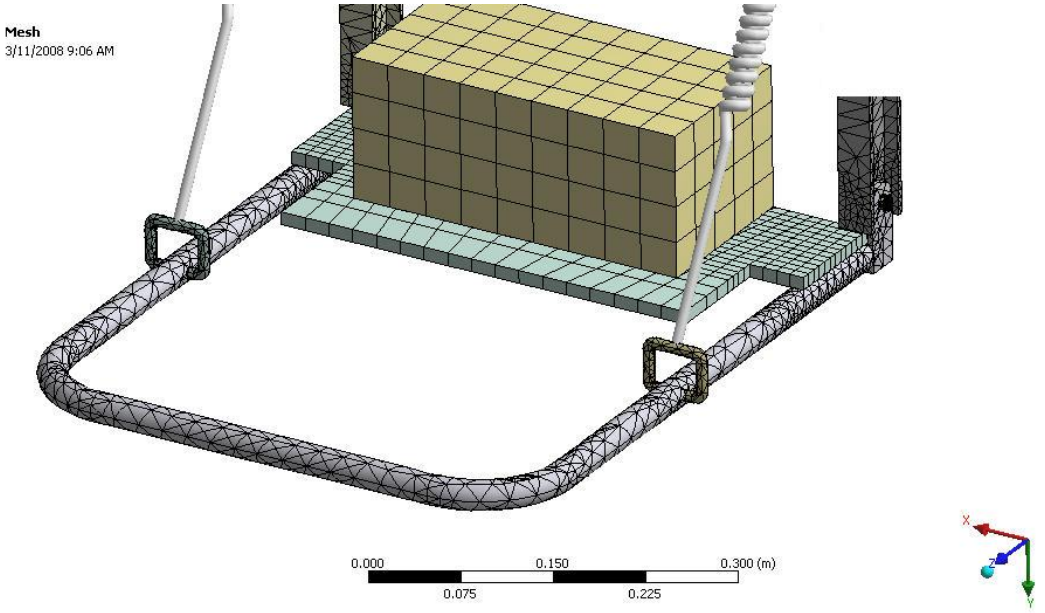

Figure 3.16: Refined mesh in lower section of seat

The complete analysis procedure is summarized in the flowchart (Figure 3.17) below,

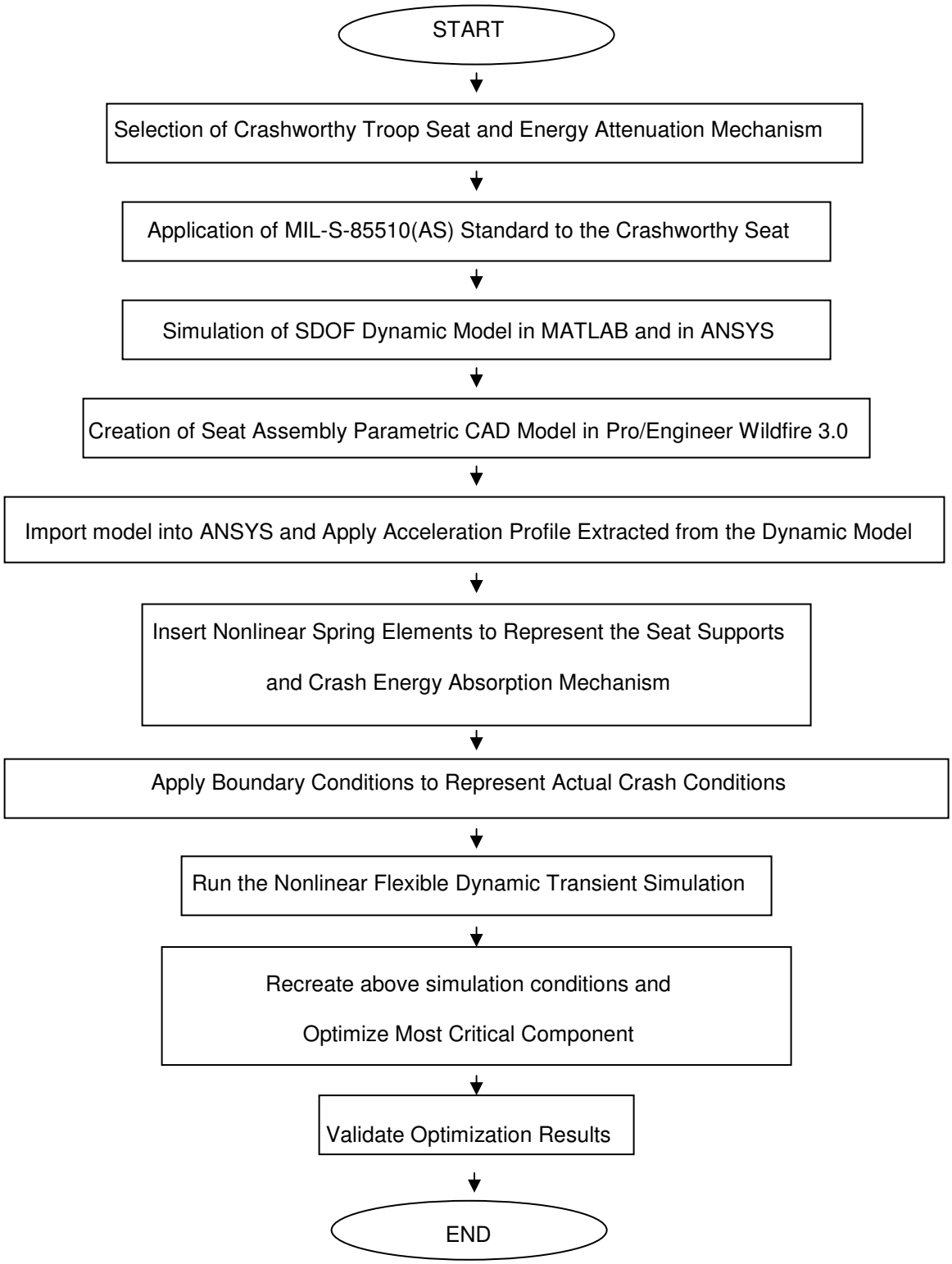

Figure 3.17: General layout of analysis procedure

3.3 Results

After adjusting the mesh size, and adding all loads and boundary conditions, the simulation was run again to obtain the final results.

Stress Results:-

All stress results shown below are at the end of the final time step i.e. at 0.068 sec. The plotted equivalent Von-Mises stress values are shown in Figure 3.18 below,

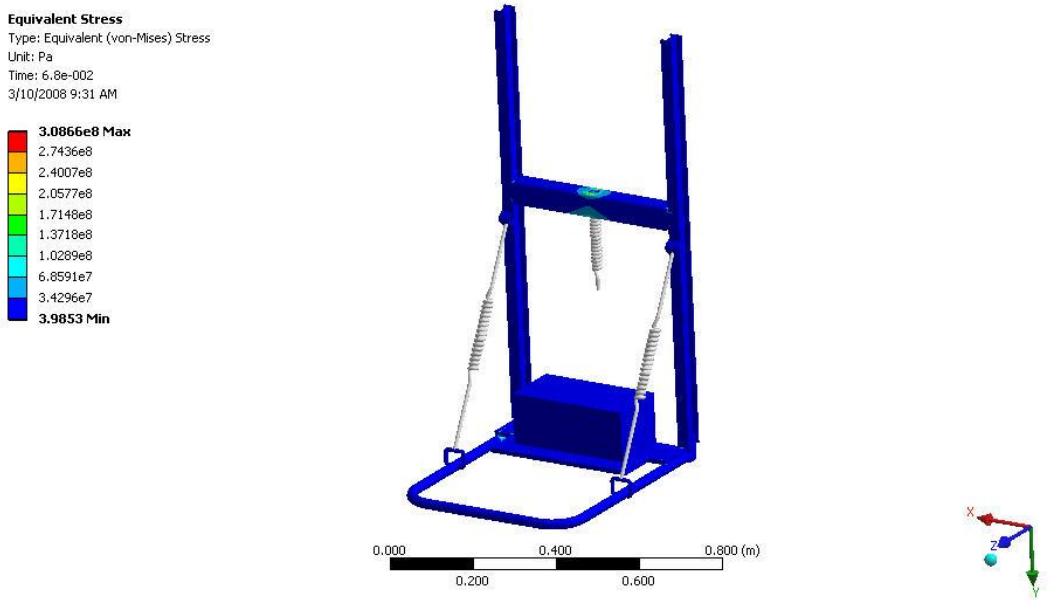

Figure 3.18: Equivalent Von-Mises stress plot for complete assembly

As expected the maximum stress was observed in the upper connection. The stress in the upper connection increases when the spring is in the first region with slope k1, and then remains constant throughout region 2 due to the sustained crushing load. This can be seen from the graph of stress vs time for the upper connection as shown in Figure 3.19,

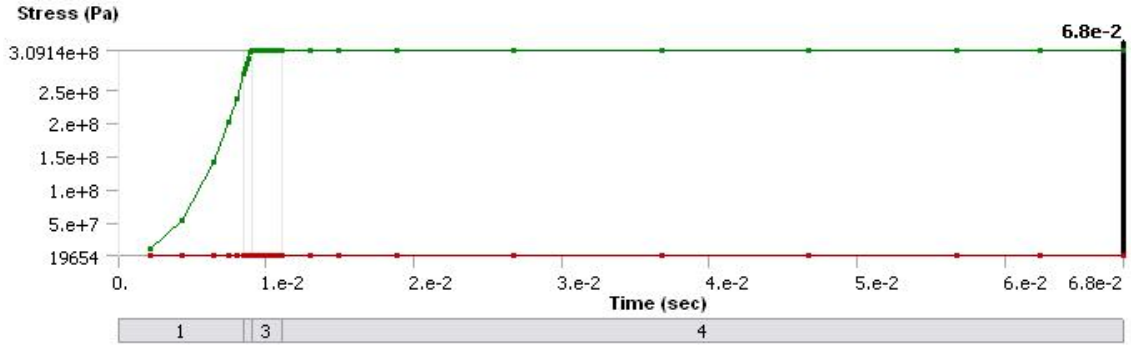

Figure 3.19: Plot of stress vs time for assembly

The stress plots for the cushion frame (Figure 3.3 (H)) and bolt at 0.068 sec is shown in Figures 3.20 and 3.21 respectively,

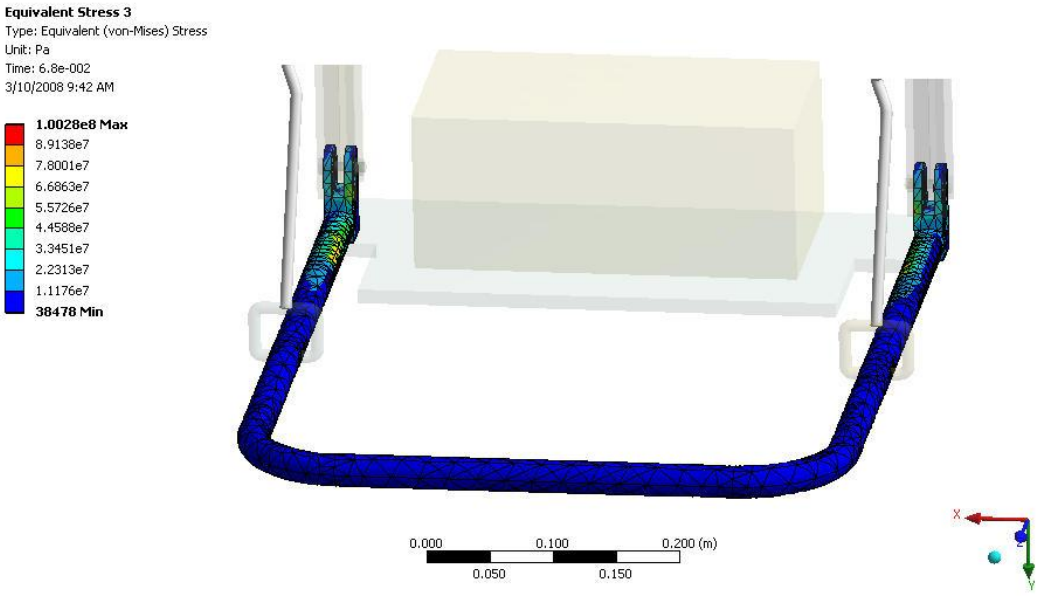

Figure 3.20: Equivalent Von-Mises stress plot for cushion frame

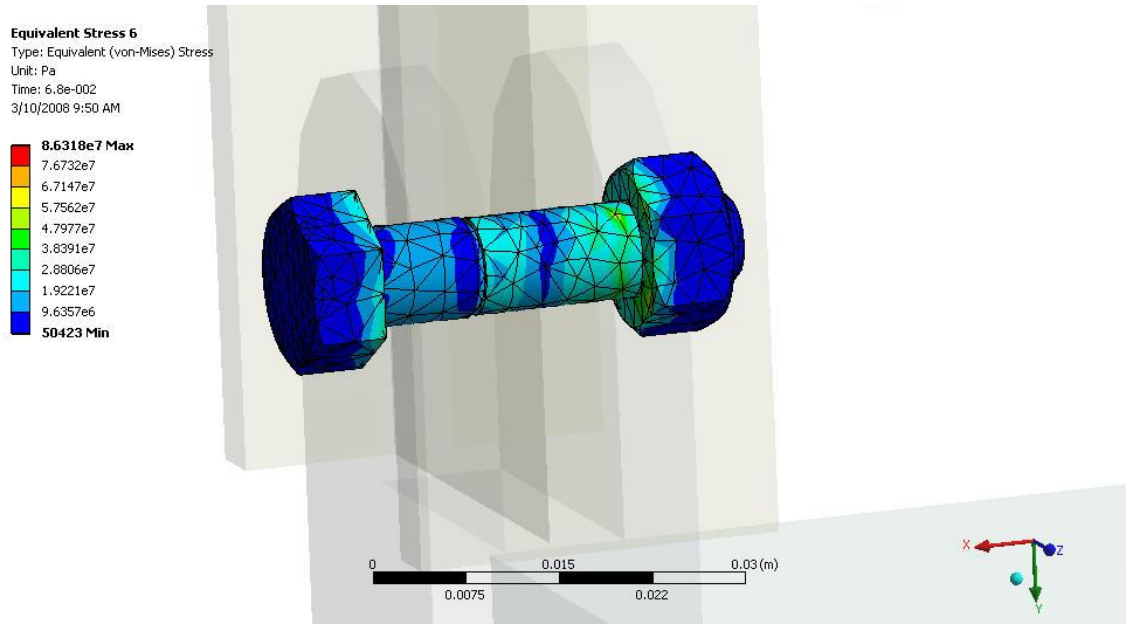

Figure 3.21: Equivalent Von-Mises stress plot for bolt

The stress in the upper and lower rings (Figure 3.3 (B and G)) decreases after the peak of the spring representing the crash tube is reached. This seems logical since before the peak is reached, inertial forces will be transmitted to the connections and when the spring enters region 2, it will offer very little resistance, thus relieving the forces on the rings. This is shown in Figures 3.22 and 3.23 below,

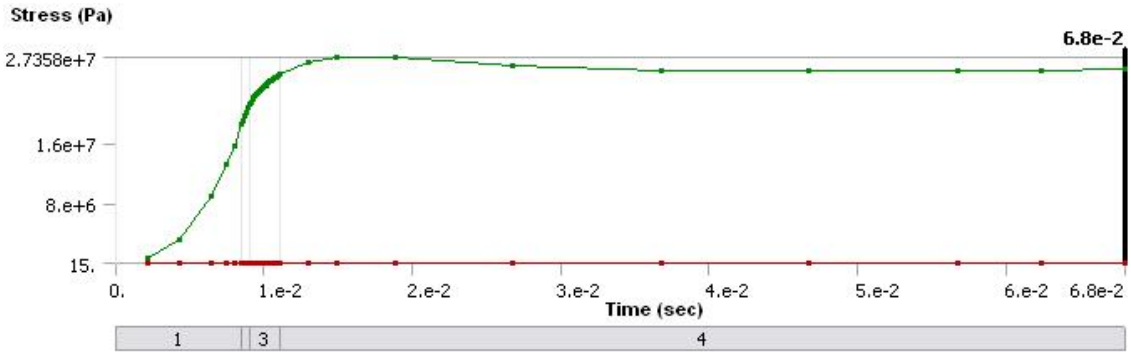

Figure 3.22: Stress vs time for lower ring

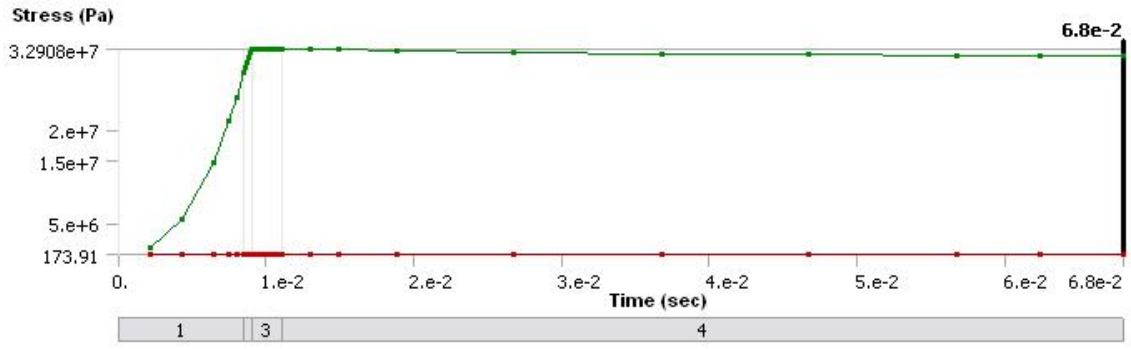

Figure 3.23: Stress vs time plot for upper ring

The stress plots for the lower and upper rings, I frame and upper connection (Figure 3.3 (G, B, C and A)) at 0.068 sec is shown in Figures 3.24, 3.25, 3.26 and 3.27 respectively,

Figure 3.24: Equivalent Von-Mises stress plot for lower rings

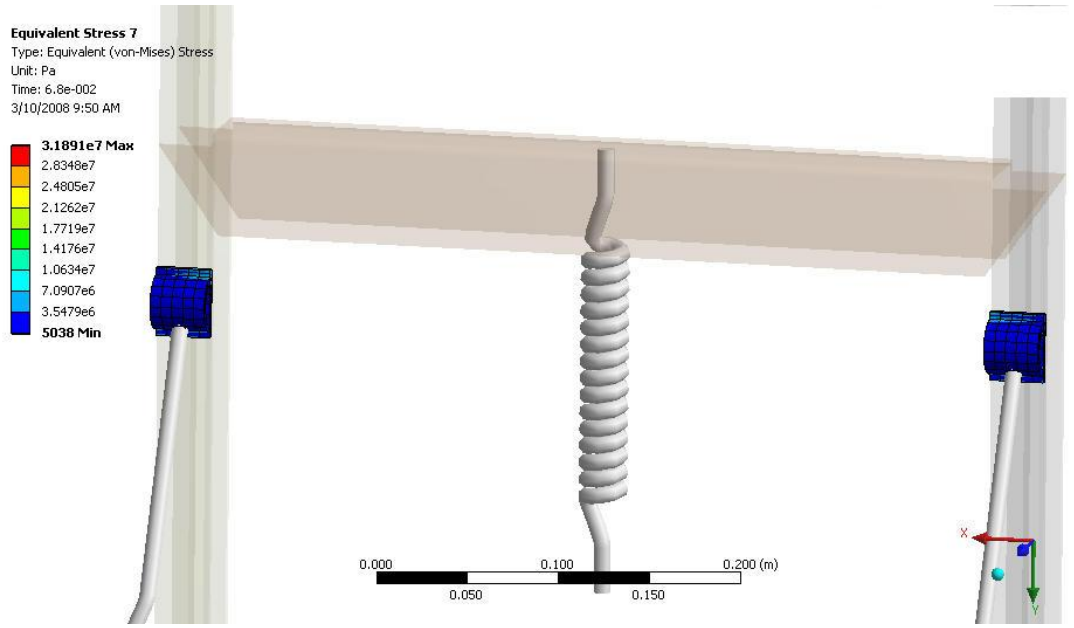

Figure 3.25: Equivalent Von-Mises stress plot for upper ring

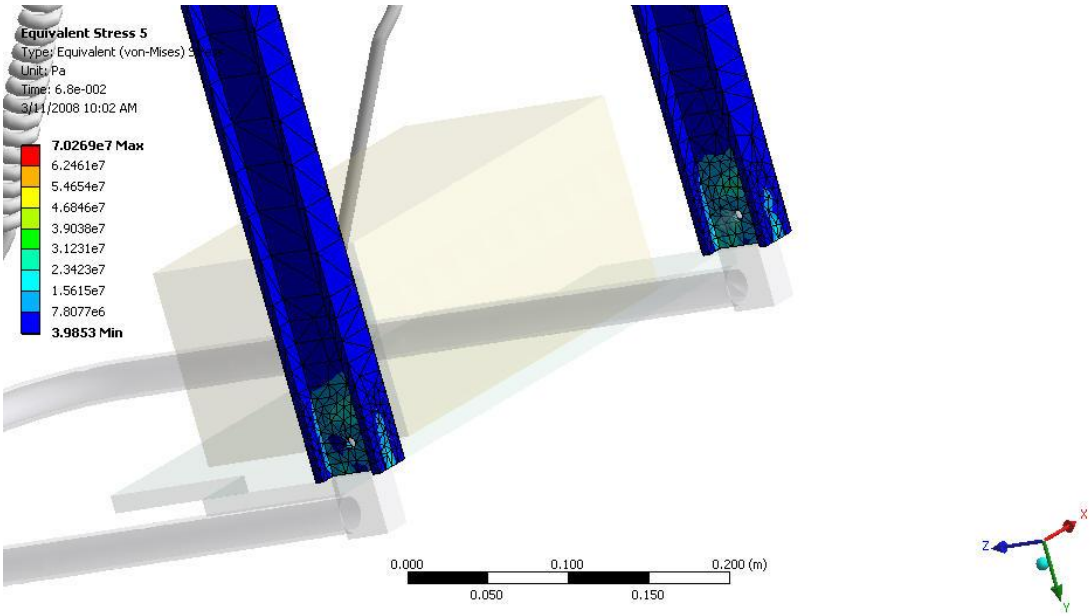

Figure 3.26: Equivalent Von-Mises stress plot for I-frame

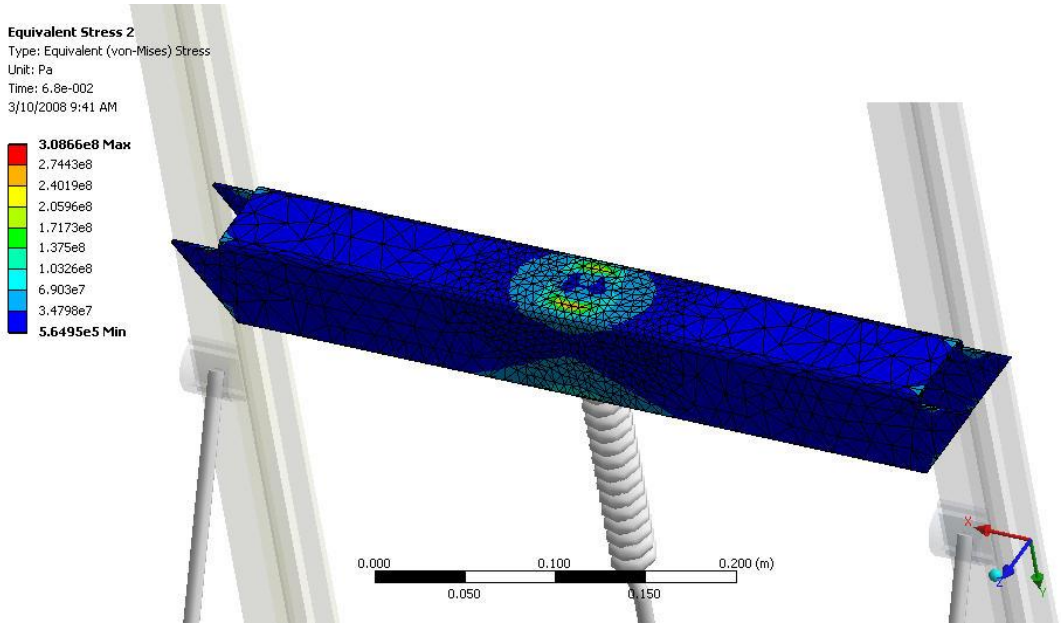

Figure 3.27: Equivalent Von-Mises stress plot for upper connection

3.2.1 Deformation Results

There is a difference of about 1.3 percent (0.00261 m) between the deformations from the ANSYS SDOF spring-mass model and the ANSYS WB simulation, while there is a difference of 2.5 percent (0.00511 m) between deformation results from the MATLAB and ANSYS WB simulations. This error could be due to the fact that all the mass may not be completely transmitted to the crash tube. The deformation plot is shown in figure 3.28,

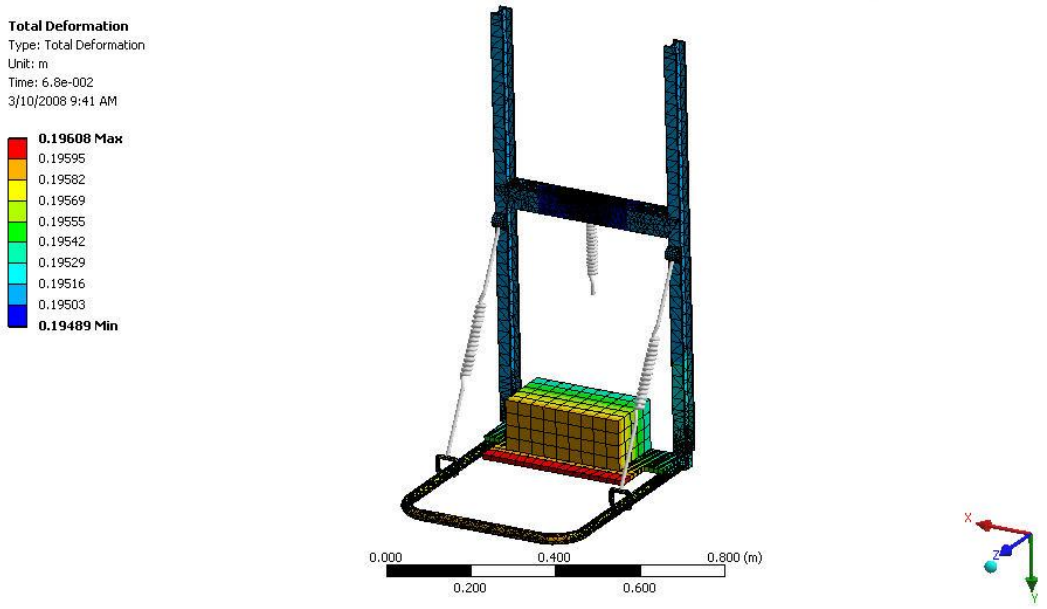

Figure 3.28: Total deformation plot of seat assembly

The stress in the Upperconnection is 308.6 MPa which is greater than its yield stress of 250 MPa, so the upper connection might not be safe. Even if Upperconnection does not fail completely, it might deform in an undesirable manner causing injury to the occupant. After observing all the stress results, it was concluded that all of the parts except the Upperconnection will not fail in a crash landing situation as all the stresses are below the yield stress of the materials.

3.2.2 Force Convergence

If a nonlinear analysis is run in ANSYS, a force convergence plot can be seen. A general contact problem is a nonlinear problem since ANSYS must iterate to determine whether the contact element status is open or closed. A plasticity analysis is also nonlinear, due to the nonlinear relationship between between stress and strain, and hence between deflection and applied load. Turning on large deflections in a structural analysis also causes ANSYS to do a nonlinear analysis. In this case, the nonlinearity is the change in stiffness with changes in deflection.

"The GST plot can provide us with useful information on the performance and success of our nonlinear analysis. The quantities being plotted are always some 'residual' vs. a tolerance. The residual can be thought of as the difference between the applied load and the calculated reaction load. Ideally we want the reaction load to match the applied load. In a linear analysis this is exactly what happens. In a nonlinear analysis, however, the Newton-Raphson technique is utilized to iterate to a solution. Without going into the details of the math, a norm, which is a scalar quantity used to express the reaction load, is compared to a norm of the applied load. When the difference between those two quantities becomes less than the tolerance, our solution is converged.

Load steps are usually applied in a simulation. Since loads are normally ramped from their initial value at the beginning of a load step to their final value at the end of a load step, each substep takes a bigger 'bite' of the load. Thus using multiple substeps allows ANSYS to tackle a smaller 'bite' of the solution at a time rather than attempting to apply the full load of a load step all at once. This generally enhances the convergence behavior, allowing us to more accurately model the load and response history, and sometimes allowing us to get a converged solution that we couldn't otherwise obtain without doing multiple substeps.

Within each substep, ANSYS will typically perform several equilibrium iterations, using the Newton-Raphson technique, to balance the reaction load with the applied load. The displacement increment is adjusted in these iterations until convergence on load is achieved. As users, we control the load steps and to a large degree the substeps, but we don't have direct control over the number of equilibrium iterations needed to obtain convergence.

As our analysis progresses, we want the Force convergence on the force convergence plot to drop below the Force criterion curve. If it does, in most cases the substep will be converged and the analysis will continue with the next substep, if any. If the norm curve does not drop below the criterion curve, or does so slowly, we need to make some adjustments to our analysis to improve its performance or at least to get it to converge.

Thus, the force convergence plot gives us a history of the convergence behavior of our nonlinear analysis. We can use this information to track how well or how poorly our solution is converging, in hopes that we can improve the performance if necessary. The knobs to turn to improve our convergence behavior will be the topic of a future article". [20] The force convergence plot for the seat impact analysis is shown in Figure 3.29.

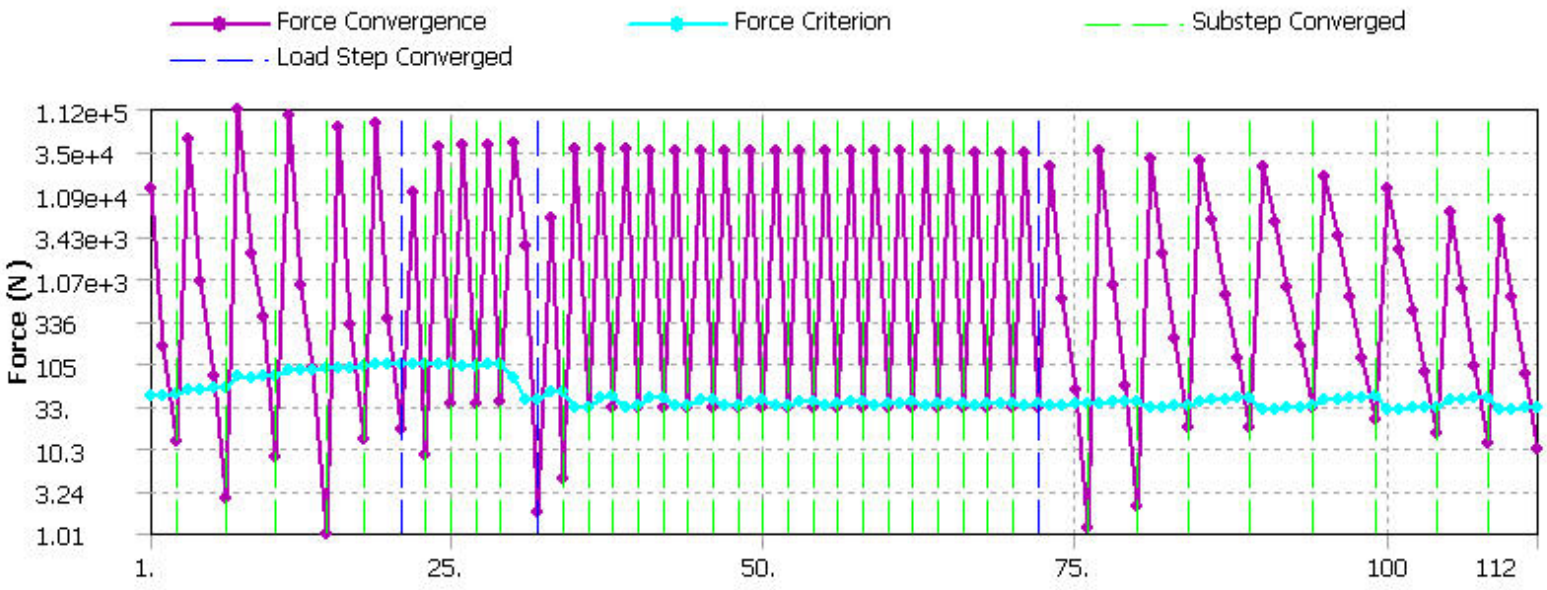

Figure 3.29: Force convergence plot

CHAPTER 4

OPTIMIZATION

4.1 Design of Experiments (DOE)

Design optimization is the engineering process that delivers the best performance with the least material weight, the smallest net volumes, or the greatest strength from a material, etc. Design of experiments (DOE) can be defined as a procedure for choosing a set of samples in the design space, with the general goal of maximizing the amount of information gained from a limited number of samples [21]. One of the goals of a typical DOE study is to estimate and predict the trends in response data. Hence response surface approximations are often associated with design of experiments (DOE) [22]. In general the DOE techniques can be classified as classical or modern DOE techniques. The classical DOE techniques were developed for laboratory and field experiments that possess random error sources while the modern DOE techniques pertain to deterministic computer simulations [22].

Examples of classical techniques are central composite design, Box-Behnken design and full- and fractional-factorial design. These classical techniques work well when the sample points are put at the extremes of the design space. Examples of modern techniques are quasi-Monte Carlo sampling, Orthogonal array sampling, Latin hypercube sampling, etc. The modern techniques are also known as space filling methods as they put the sampling points in the inner space as compared to the extremes of the design space in order to accurately extract the response trend information [23].

The ANSYS Workbench DesignXplorer solution works from within the ANSYS Workbench interface to perform Design of Experiments (DOE) analyses of any ANSYS Workbench simulation with defined parameters.

4.2 Goal Driven Optimization (GDO)

Goal Driven Optimization (GDO) is a constrained, multi-objective optimization (MOO) technique in which the "best" possible designs are obtained from a sample set given the goals set for the design parameters. The sample set is generated by screening the sample generation menu. The GDO process allows one to determine the effect on input parameters with certain preferences applied for the output parameters [19].

For example, in a structural engineering design problem, one may want to determine which set of designs (in terms of geometric problem dimensions and material types) best satisfy minimum mass, maximum natural frequency, maximum buckling and shear strengths, and minimum cost, with maximum value constraints on the von Mises stress and maximum displacement [19].

GDO can be used for design optimization in two ways: the Screening approach or the Advanced approach. The Screening approach is a non-iterative direct sampling method by a quasi-random number generator based on the Hammersley algorithm. The Advanced approach is an iterative Multi-objective Genetic Algorithm (MOGA), which can optimize problems with continuous input parameters [19].

For ANSYS DesignXplorer the procedure for optimization can be summarized in the following steps.

1. Run a simulation in ANSYS Workbench and record the input and output parameters.
2. Through DesignXplorer central composite DOE scheme create candidate designs (Automatic design points).
3. Create response surfaces using second order polynomial based regression analysis with the candidate designs and the true responses.
4. Define design goals for the optimization such as allowable constraints etc.
5. Create new design points through sample generation from the specified goals [22].

4.3 Setup and Results

The seat assembly can be optimized as a whole but this would prove to be a very time consuming and computationally intensive task as each run takes about 1 hour and 35 minutes using a Pentium 4 CPU, with 3.00 GHz and 3 GB RAM. Instead the approach adopted here is to isolate the most critical part in the assembly and replicate the conditions using the data from the simulation of the complete seat.

The part selected for optimization is the upperconnection since it is the only part in which the stress exceeds the yield stress (Yield Stress for Steel = 250 MPa). Similar loading conditions can be replicated on this part by applying appropriate boundary conditions. These conditions were created by inserting a nonlinear spring with the same real constants that were used in the case of the seat assembly simulation and by restricting the edges in the X and Y directions (Figure 4.2).

Figure 4.1: Input displacement vs time profile

The motion of the upperconnection (Figure 3.3 (A)) is duplicated by applying a displacement profile to upperconnection as shown in Figure 4.1. This displacement represents the actual displacement of the upperconnection as determined from simulation of the complete seat assembly. A summary of the applied loads and boundary conditions is shown in Figure 4.2,

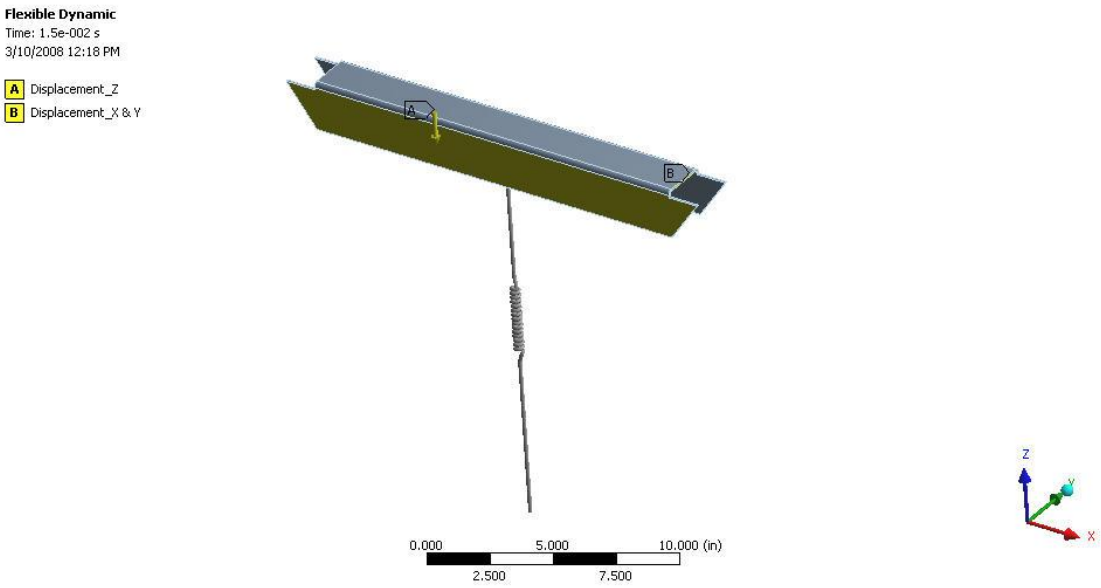

Figure 4.2: Applied loads and boundary condition

After the simulation was run with the above conditions, the following stress distribution was obtained at 0.068 sec,

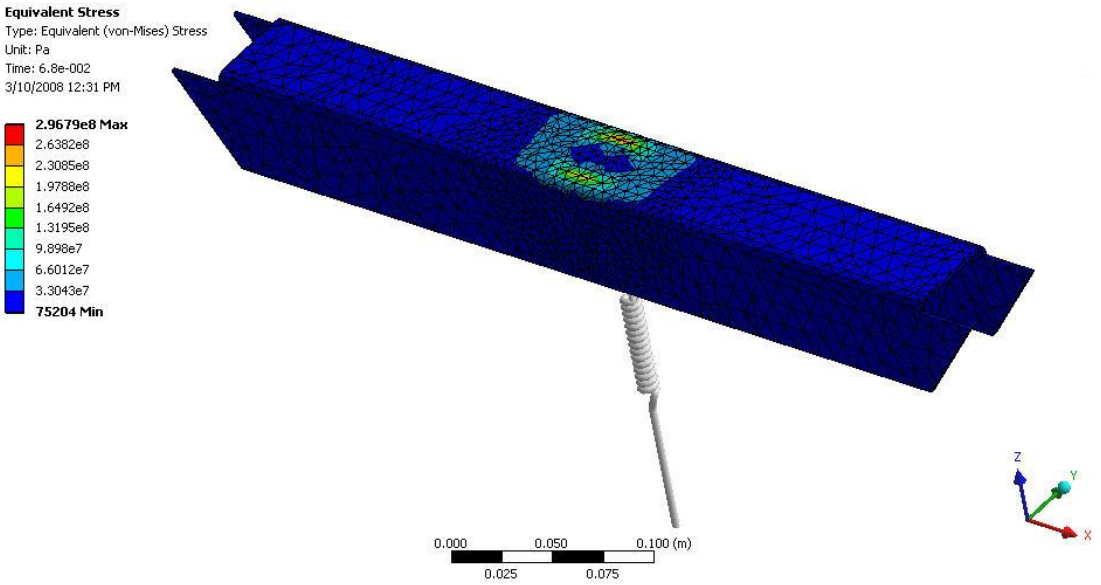

Figure 4.3: Equivalent Von-Mises stress plot for upper connection

The maximum stress on upperconnection is 2.9679e8 Pa from the isolated run, and it is 3.0866e8 Pa when part of the actual assembly at 0.068 sec. From the above stress distribution plot it is evident that this setup creates forces on the seat that closely match the forces on the part in the actual simulation as the difference is only 3.05 percent.

Parameters selected for optimization of the Upperconnection are upperlength_DS, upperconthick_DS and upperconnwidth_DS as shown in Figure 4.4 below,

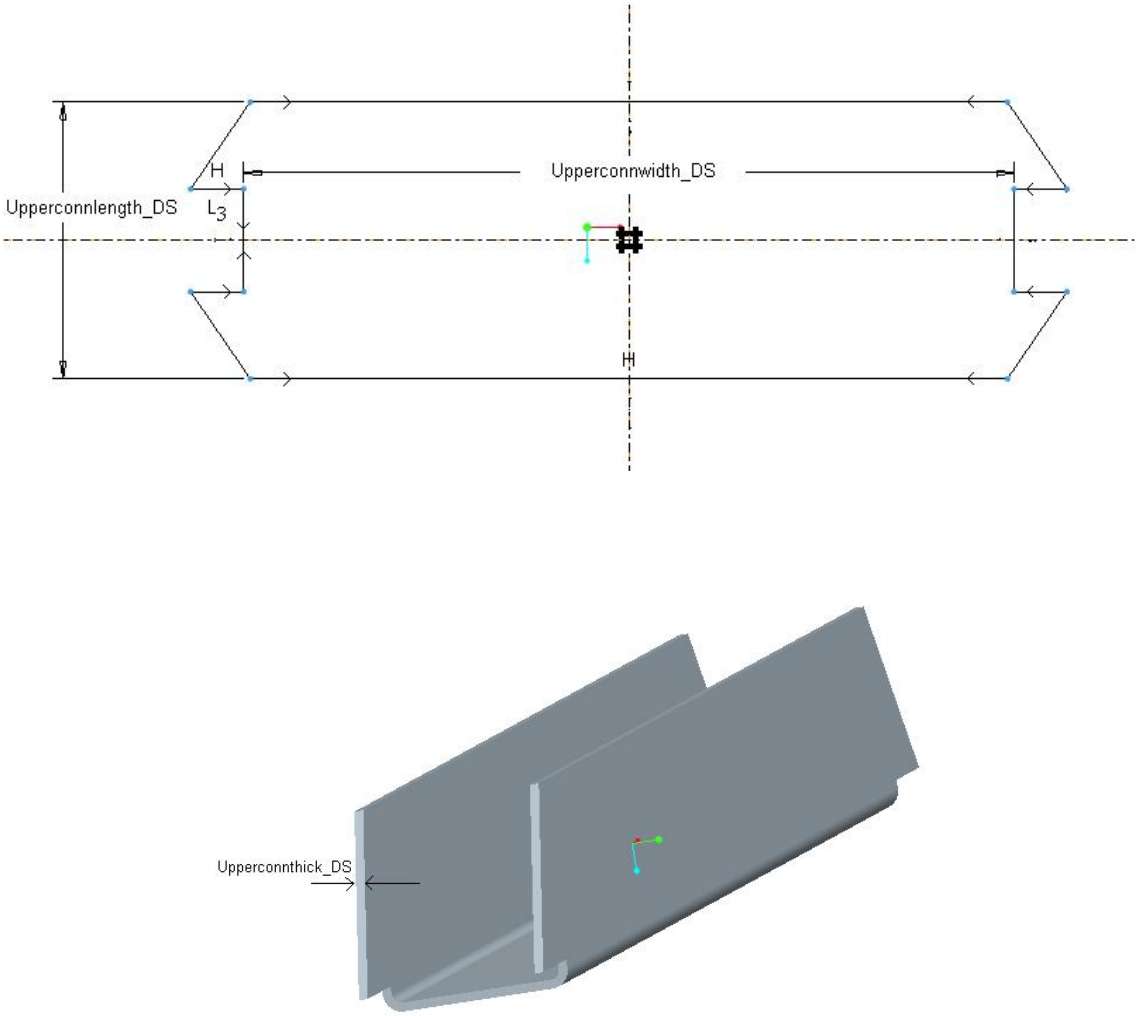

Figure 4.4: Parameters selected for optimization

Lower and upper bound limits were set on the above mentioned parameters (Figure 4.8), simulation parameter type was set to design variable, parameter classification was set to continuous, and Design of Experiments was used to process the DOE designs. The generated response surfaces for the three CAD parameters and equivalent stress are shown in Figures 4.5, 4.6 and 4.7.

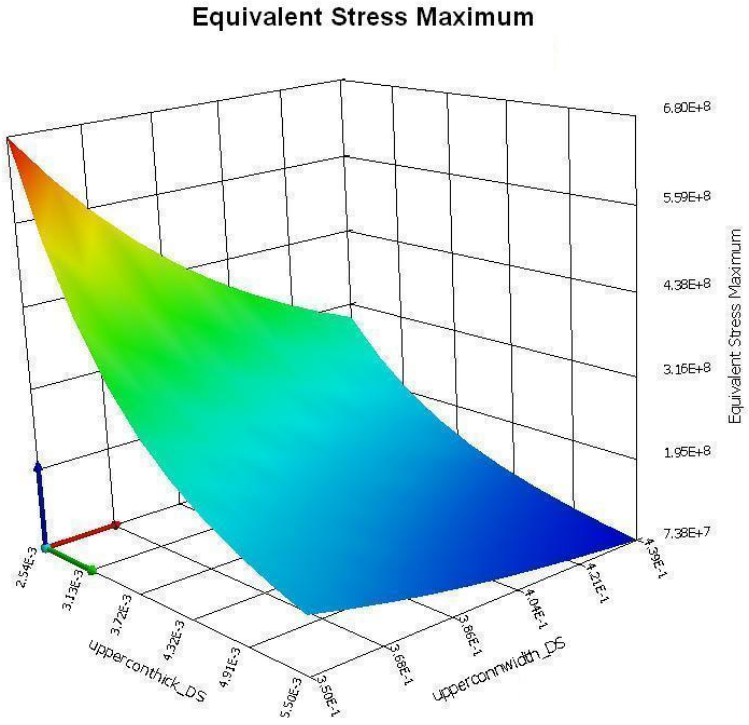

Figure 4.5: Response plot for upperconnection width

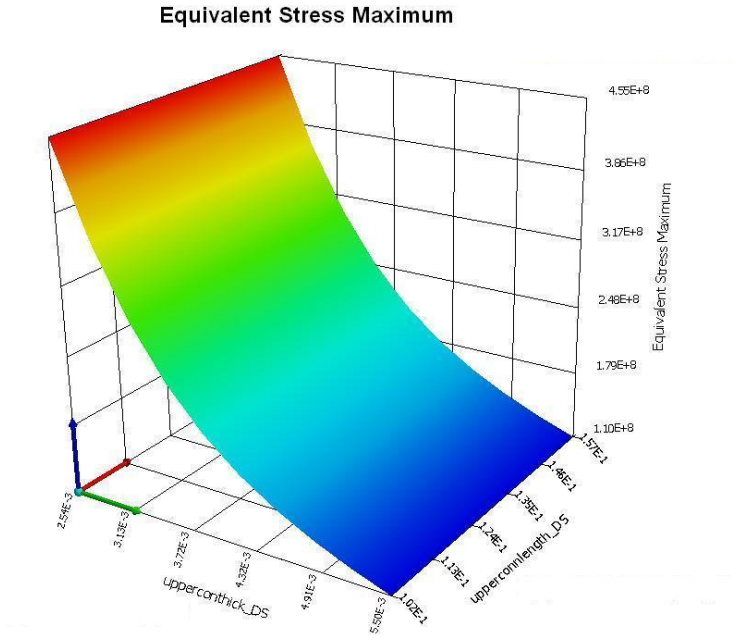

Figure 4.6: Response plot for upperconnection thickness

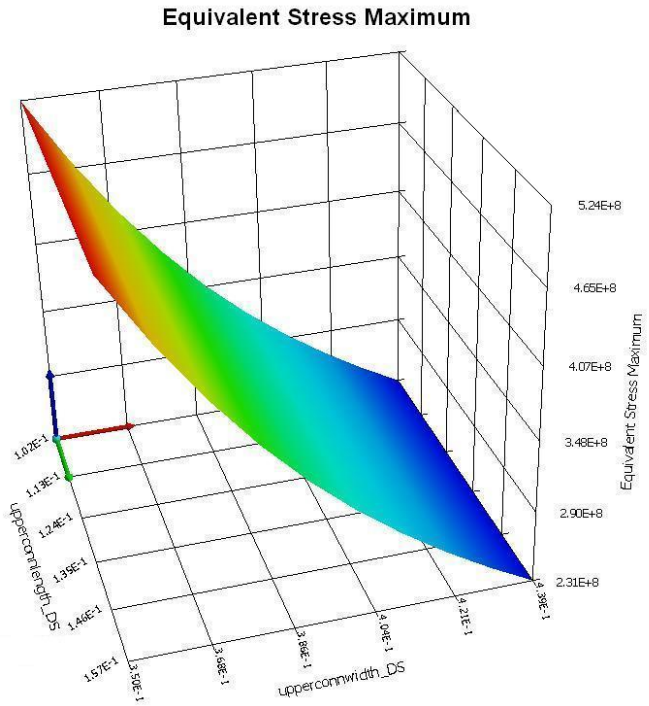

Figure 4.7: Response plot for upperconnection length

The input and response parameter goals are shown in Figure 4.8,

Input Parameter Goals

Click rows in this table to assign design goals to input parameters.

Name	Lower Bound	Upper Bound	Target	Desired Value	Importance
upperconnwidth_DS	0.35	0.43937		Near Lower Bound	Default
upperconnlength_DS	0.1016	0.15748		Near Midpoint	Default
upperconthick_DS	2.54e-003	5.5e-003		No Preference	Default

Response Parameter Goals

Click rows in this table to assign design goals to response parameters. Defining a target value is optional.

Name	Target	Desired Value	Importance	TradeOff
Equivalent Stress Maximum	2.e+008 Pa	Near Target	Higher	On

Figure 4.8: Parameter goals

The results obtained for this problem using the ANSYS DesignXplorer goal driven optimization process is given in Figure 4.9,

Candidate Designs

Generate or update candidate designs based on the current goals

Parameter	Candidate A		Candidate B		Candidate C	
upperconnwidth_DS	0.39347	★★★	0.38318	★★	0.37546	★★
upperconnlength_DS	0.10177	★★★	0.10192	★★★	0.10265	★★★
upperconthick_DS	3.8647e-003	★★★	4.0416e-003	★★★	3.9983e-003	★★★
Equivalent Stress Maximum	1.9949e+008 Pa	★★★	2.0103e+008 Pa	★★★	2.2039e+008 Pa	★★★

Figure 4.9: Results from ANSYS DesignXplorer goal driven optimization

Candidate A is selected as the new design since it is rated the best amongst the three and gives the lowest value of equivalent stress. A comparison of the original and updated model parameters shows us that the volume, mass and stress is reduced, thus proving to be a very good design. This is illustrated in Table 4.1 below,

Table 4.1: Dimensions before and after optimization

	Original Part (m)	Optimized Part (m)
Upperconnection width	0.4393	0.39347
Upperconnection length	0.15748	0.10177
Upperconnection thickness	0.00254	0.003864

A comparison in Table 4.2 shows us that the volume and mass are reduced by 7.51 percent

Table 4.2: Reduction in volume and mass

	Original Part	Optimized Part
Volume (m^3)	1.8402e-4	1.7023e-4
Mass (kg)	1.4445	1.336

4.4 Validation

Since the part was isolated from the seat assembly for the purpose of optimization, the updated part was placed in the assembly to determine if the stresses are indeed lowered. The results of the simulation for the updated system are shown in Figure 4.10,

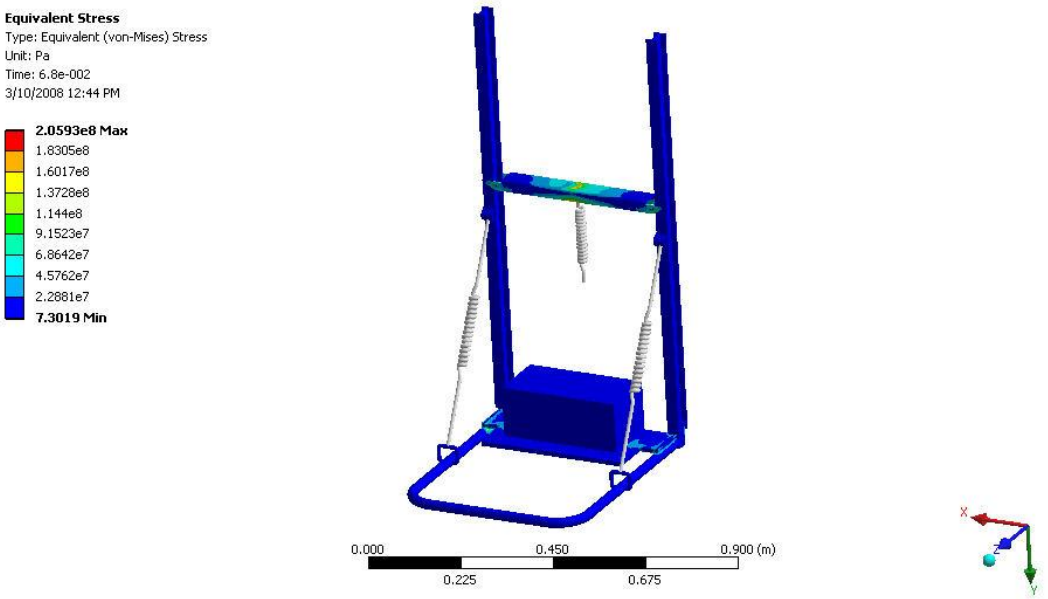

Figure 4.10: Equivalent Von-Mises stress plot for optimized seat assembly

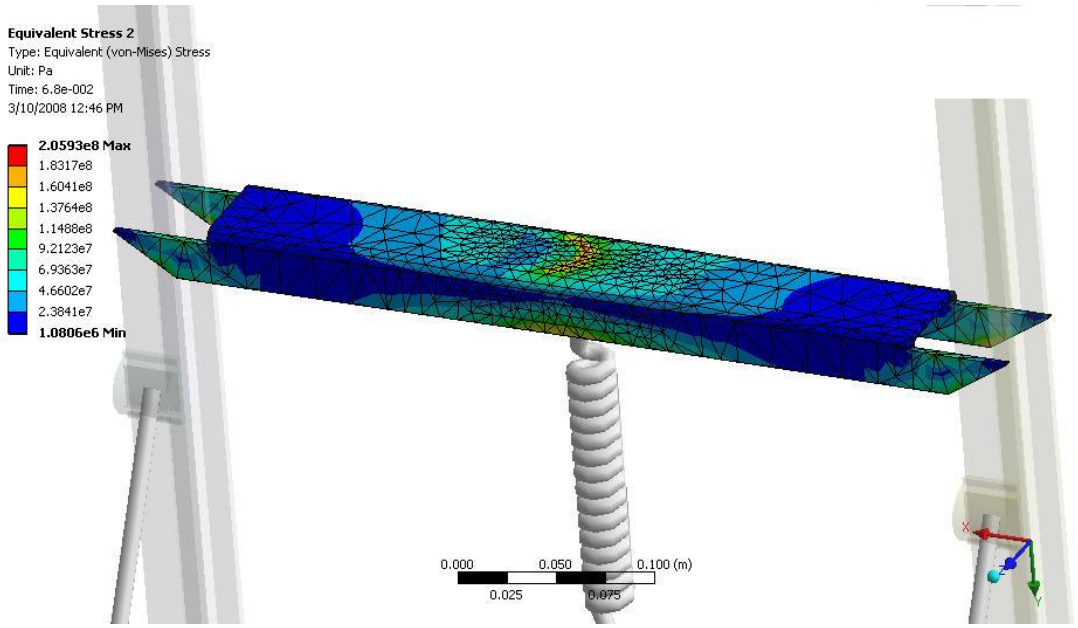

Figure 4.11: Equivalent Von-Mises stress plot for optimized upper connection

The maximum stress according to DesignXplorer Goal Driven Optimization (GDO) is 1.9949e8 Pa while the simulation results show that the maximum stress is 2.059e8 Pa (figure 4.11). So the error between the two is very small and is of the order of 3 percent thus validating the optimized design.

CHAPTER 5

CONCLUSIONS AND RECOMMENDATIONS

5.1 Introduction

The main objective of this research was to analyze a crashworthy helicopter seat using ANSYS, a powerful finite element solver. Usually the approach for such an FEA analysis would be to perform a drop test simulation, but this approach would be very time and computationally intensive. So a different approach towards the analysis was taken here so that it could be solved using MATLAB and the capabilities of ANSYS v11.0. After the analysis was carried out, an optimization of the critical component was carried out using the ANSYS inbuilt Design of Experiments (DOE), Goal Driven Optimization (GDO) method.

5.1.1 Conclusions

After carrying out the transient dynamic nonlinear impact simulation in ANSYS Workbench, it was observed that the stress levels in all parts of the assembly except the upperconnection (Figure 3.3 (A)) is under high stress and could possibly fail. This part was optimized using goal driven optimization and the stress levels were reduced along with a reduction in the mass. From the response plots it was clear that the thickness had the maximum impact on the stress levels followed by the width and the length of the component. By reattaching the part in the assembly and running the simulation again, it was validated that the stress values had actually reduced, thus providing a better design.

5.1.2 Recommendations

1. Since the problem is a complex dynamic problem in nature and very time and computationally intensive, it was not feasible to optimize the complete assembly. But this can be achieved and all the parts of the seat can be optimized to reduce weight.

2. Since the problem carried out was complex in nature, it was very difficult to find actual test data for stress levels in the components of the seat, so one could verify these results by carrying out an actual drop test simulation in a lab.

3. A mass block was used to represent the weight of the 50th percentile U.S. Army male aviator. This can be replaced with a model of an anthropometric dummy with the appropriate dimensions. This would provide a much more realistic weight distribution of the occupant

APPENDIX A

MATLAB M-FILES

A.1 SDOF dynamic model in MATLAB

In this appendix the MATLAB file used for the SDOF spring-mass impact simulation is shown.

Range-Kutta fourth order method is applied using the ODE45 solver.

---
1 – File main.m

```
global gm tp m k1 k2 k_cutoff

gm=      370
tp=      0.068
m=       83
k1=      11682933.7
k2=      8902.39
k_cutoff=0.000762
minstep=1.00E-15
maxstep =0.0005
tstop    =0.068

init_state=[0,0,0,0]';
sim_interval = [0,tstop];

[t_ode,state]=ode45('x_dot',sim_interval,init_state);
figure

% Develop acceleration curves for plotting since only d and v are in the solution
aman=zeros(size(t_ode)) % acceleration of man
delta = state(:,3) - state(:,1)
aplane=zeros(size(t_ode))
for index = 1 : length(t_ode)
  % Calculate aman(index)
  if delta(index) < k_cutoff
    aman(index) = k1 * delta(index) / m
  else
    aman(index) = k2 / m
  end
  % Calculate aplane(index)
  if t_ode(index) < tp / 2
      aplane(index)= gm / (tp / 2) * t_ode(index)
  elseif t_ode(index) < tp
      aplane(index) = 2 * gm - gm / (tp / 2) * t_ode(index)
  else
      aplane(index) = 0
  end
end

% Plot accelerations
figure(1);
plot(t_ode,aman,'r',t_ode,aplane,'b');
```

```
title('ACCEL VS TIME');
xlabel('Time (sec)');
ylabel('Acceleration (m/s/s)');

% plot velocities
figure(2);
plot(t_ode,state(:,2),'r',t_ode,state(:,4),'b');
title('VELOCITIES VS TIME');
xlabel('Time (sec)');
ylabel('Velocity (m/s)');

% plot displacements
figure(3);
plot(t_ode,state(:,1),'r',t_ode,state(:,3),'b');
title('DISPLACEMENTS VS TIME');
xlabel('Time (sec)');
ylabel('Displacement (m)');
```

---

2 – Function x_dot.m

```
function state_dot = x_dot_h4(t,x); % x_dot.m
global gm tp m k1 k2 k_cutoff

% Input of this function is time t and state variable x
% Output of this function is state_dot which is calcualted time derivative of x

% state variables:
  % x1 is displacement of man
  % x2 is velocity of man
  % x3 is displacement of the plane
  % x4 is velocity of the plane.

% Derivatives of state variables:
  % dx1/dt = x2

  % dx2/dt = (1/Mman) * Fspring = (1/Mman) * f(delta)
  % f is nonlinear spring function
  % f(delta1) = k1*x1 for delta<k_cutoff, k2 for delta1>k_cutoff
  % delta = x3-x1 is the compression of the spring

  % dx3/dt = x4

  % dx4/dt = acceleration of plane = triangle pulse = given function of time


% initialize state dot as a column vector of dimension 4
state_dot=zeros(4,1);

% find dx1/dt
```

```
state_dot(1) = x(2) % dx1/dt = x2

% Find dx2/dt
delta = x(3) - x(1)
if delta < k_cutoff
  state_dot(2) = k1 * delta / m
else
  state_dot(2) = k2 / m
end

% find dx3/dt
state_dot(3) = x(4)

% find dx4/dt - the triangle function
if t < tp / 2
  state_dot(4) = gm / (tp / 2) * t
elseif t < tp
  state_dot(4) = 2 * gm - gm / (tp / 2) * t
else
  state_dot(4) = 0
end
% find dx4/dt - the triangle function
if t < tp / 2
  state_dot(4) = gm / (tp / 2) * t
elseif t < tp
  state_dot(4) = 2 * gm - gm / (tp / 2) * t
else
  state_dot(4) = 0
end
```

A.2 Orthotropic material properties for I-frame

This appendix shows the MATLAB M-file which uses lamination theory to find the orthotropic elastic material properties of the Cr/Ep I-frame.

```
format long
%Material Properties
E1=147e9
E2=10.3e9
E3=10.3e9
G12=7e9
G23=3.7e9
G13=7e9
v12=0.27
v23=0.54
v13=0.27
tply=6.35e-4
t=0.00508
v21=(v12*E2)/E1;
Q11=E1/(1-v12*v21);
Q12=(v12*E2)/(1-v12*v21);
Q16=0;
Q22=E2/(1-v12*v21);
Q66=G12;
Q26=0;
Q=[Q11 Q12 Q16;Q12 Q22 Q26;Q16 Q26 Q66];


%Calculation of Qbar matrix for +45 degrees
m1=cos(pi/4)
n1=sin(pi/4)
Q11a=m1^4*Q11+n1^4*Q22+2*(Q12+2*Q66)*m1^2*n1^2;
Q22a=n1^4*Q11+m1^4*Q22+2*(Q12+2*Q66)*m1^2*n1^2;
Q12a=m1^2*n1^2*(Q11+Q22-4*Q66)+(m1^4+n1^4)*Q12;
Q16a=m1^3*n1*(Q11-Q12-2*Q66)-m1*n1^3*(Q22-Q12-2*Q66);
Q26a=m1*n1^3*(Q11-Q12-2*Q66)-m1^3*n1*(Q22-Q12-2*Q66);
Q66a=m1^2*n1^2*(Q11+Q22-2*Q12-2*Q66)+(m1^4+n1^4)*Q66;
Q21a=Q12a;
Qbar45=[Q11a Q12a Q16a;Q21a Q22a Q26a;Q16a Q26a Q66a]
%Calculation of Qbar matrix for -45 degrees
m2=cos(-pi/4)
n2=sin(-pi/4)
Q11b=m2^4*Q11+n2^4*Q22+2*(Q12+2*Q66)*m2^2*n2^2;
Q22b=n2^4*Q11+m2^4*Q22+2*(Q12+2*Q66)*m2^2*n2^2;
Q12b=m2^2*n2^2*(Q11+Q22-4*Q66)+(m2^4+n2^4)*Q12;
Q16b=m2^3*n2*(Q11-Q12-2*Q66)-m2*n2^3*(Q22-Q12-2*Q66);
Q26b=m2*n2^3*(Q11-Q12-2*Q66)-m2^3*n2*(Q22-Q12-2*Q66);
Q66b=m2^2*n2^2*(Q11+Q22-2*Q12-2*Q66)+(m2^4+n2^4)*Q66;
Q21b=Q12b;
Qbar_45=[Q11b Q12b Q16b;Q21b Q22b Q26b;Q16b Q26b Q66b]
```

```
h0=-2.54e-3
h1=-1.905e-3
h2=-1.27e-3
h3=-6.35e-4
h4=0
h5=6.35e-4
h6=1.27e-3
h7=1.905e-3
h8=2.54e-3
%ABD matirx
A=Qbar45*(h1-h0)+Qbar_45*(h2-h1)+Qbar45*(h3-h2)+Qbar_45*(h4-h3)+Qbar_45*(h5-
h4)+Qbar45*(h6-h5)+Qbar_45*(h7-h6)+Qbar45*(h8-h7)
B=(1/2)*(Qbar45*(h1^2-h0^2)+Qbar_45*(h2^2-h1^2)+Qbar45*(h3^2-h2^2)+Qbar_45*(h4^2-
h3^2)+Qbar_45*(h5^2-h4^2)+Qbar45*(h6^2-h5^2)+Qbar_45*(h7^2-h6^2)+Qbar45*(h8^2-h7^2))
D=(1/3)*(Qbar45*(h1^3-h0^3)+Qbar_45*(h2^3-h1^3)+Qbar45*(h3^3-h2^3)+Qbar_45*(h4^3-
h3^3)+Qbar_45*(h5^3-h4^3)+Qbar45*(h6^3-h5^3)+Qbar_45*(h7^3-h6^3)+Qbar45*(h8^3-h7^3))
ABD=[A B;B D]
abd=inv(ABD)
%Calculate material properties
EY=1/((abd(1,1))*t)
EZ=1/((abd(2,2))*t)
niuyz=-(abd(2,1)/abd(1,1))
Gzy=1/((abd(3,3))*t)
```

APPENDIX B

ANSYS APDL FILES

B.1 SDOF dynamic model in ANSYS

In this appendix the ANSYS APDL file used for the SDOF simulation is shown. The elements used are MASS21 and COMBIN39.

```
finish
/clear

/title, Integrate Accelerations to Get Displacments

max_G   = 370         ! Max Value of Accel Pulse
Pulse_t = 0.068       ! Width of Pulse (sec)

nrow = 1000

*dim, Agrd, TABLE, nrow, 2,, TIME              ! Grd Accel
*dim, Vgrd, TABLE, nrow, 2,, TIME              ! Grd Velocity
*dim, Dgrd, TABLE, nrow, 2,, TIME              ! Grd Disp

! Fill TABLES - Time Column w/Time
*vfill, Agrd(1,0), RAMP, 0.0, (Pulse_t/nrow)      ! Fill Time in Column
 Zero
*vfill, Vgrd(1,0), RAMP, 0.0, (Pulse_t/nrow)      ! Fill Time in Column
 Zero
*vfill, Dgrd(1,0), RAMP, 0.0, (Pulse_t/nrow)      ! Fill Time in Column
 Zero

*vlen,  500
*vfill, Agrd(1,1),   RAMP, 0.0,   max_G/(nrow/2)  ! Fill Acceleration
*vfill, Agrd(501,1), RAMP, max_G,-max_G/(nrow/2)  ! Fill Acceleration

*voper, Vgrd(1,1), Agrd(1,1), INT1, Agrd(1,0)     ! Integrate wrt Time
 -> Vel
*voper, Dgrd(1,1), Vgrd(1,1), INT1, Vgrd(1,0)     ! Integrate wrt Time
 -> Disp


/COM,  Plot the Acceleration Pulse
/gcolumn, 1, Acceleration
*vplot, Agrd(1,0) ,Agrd(1,1)
/wait, 2

! Plot velocity profile
/gcolumn, 1, Velocity
*vplot, Vgrd(1,0) , Vgrd(1,1)
/wait, 2

! Plot displacement profile
/gcolumn, 1, Displacement
*vplot, Dgrd(1,0) , Dgrd(1,1)
/wait, 2
```

```
/TITLE, CRASH IMPULSE SIMULATION
/PREP7
M  = 83 ! Mass of seat plus occupant

! Define nonlinear spring element
ET, 1, COMBIN39
!*
KEYOPT, 1, 1, 0
KEYOPT, 1, 2, 0
KEYOPT, 1, 3, 0
KEYOPT, 1, 4, 0
KEYOPT, 1, 6, 1
!*
!*
ET, 2, MASS21,,, 4
R, 1, 0.000762, 8899.48, 0.254, 8899.48

! Force deflection curve for COMBIN39 element

!
!            #
!            #
!            #
!            #
!            #     **********************************
!  Force     #    *
!            #   *
!            #  *
!            # *
!            #*
!            ########################################
!                     Deflection

R, 2, M
N, 1, 0    ! Ground
N, 2, 0.7  ! Mass
TYPE, 1 $ REAL, 1 $ E, 1, 2
TYPE, 2 $ REAL, 2 $ E, 2
FINISH

/SOLU
ANTYPE, TRANS
TRNOPT, FULL
NLGEOM,1
D, ALL,   UY,   0
D,   1, Ux, %Dgrd%

DELTIM, 0.0001
TIME, 0.068
OUTRES, NSOL, ALL
```

```
SOLVE
FINISH

/POST26
NUMVAR, 200
NSOL, 2, 2, U, X, Ux_Mass
NSOL, 3, 1, U, X, Ux_Aircraft floor

ABS,  2, 2,,, Ux_1
ABS,  3, 3,,, Ux_2

! ADD,  4, 2, 3, ,Ux1-Ux2 , , ,-1, 1,1,

/GRID, 1
/AXLAB, Y, DISPLACEMENT
PLVAR, 2, 3, 4
```

B.2 ANSYS Workbench command snippets

In this appendix the ANSYS APDL commands inserted to convert the linear ANSYS Workbench springs into nonlinear springs.

Command used for crash tube,

```
et,_sid,COMBIN39,0,0,2,0,,1
r,_sid,0.000762,8902.39,0.254,8902.39
```

Command used for seat supports,

```
et,_sid,COMBIN39,0,0,2,1,,1
r,_sid,0.04,4000,0.14859,4800,0.245,11300
```

A brief description of the keyopts used is given below,

KEYOPT(1)
Unloading path:
0 -- Unload along same loading curve
1 -- Unload along line parallel to slope at origin of loading curve

KEYOPT(2)
Element behavior under compressive load:
0 -- Compressive loading follows defined compressive curve (or reflected tensile curve if not defined)
1 -- Element offers no resistance to compressive loading
2 -- Loading initially follows tensile curve then follows compressive curve after buckling (zero or negative stiffness)

KEYOPT(3)
Element degrees of freedom (1-D) (KEYOPT(4) overrides KEYOPT(3)):
0, 1 -- UX (Displacement along nodal X axes)
2 -- UY (Displacement along nodal Y axes)
3 -- UZ (Displacement along nodal Z axes)
4 -- ROTX (Rotation about nodal X axes)
5 -- ROTY (Rotation about nodal Y axes)
6 -- ROTZ (Rotation about nodal Z axes)
7 -- PRES
8 -- TEMP

KEYOPT(4)
Element degrees of freedom (2-D or 3-D):
0 -- Use any KEYOPT(3) option
1 -- 3-D longitudinal element (UX, UY and UZ)
2 -- 3-D torsional element (ROTX, ROTY and ROTZ)
3 -- 2-D longitudinal element. (UX and UY) Element must lie in an X-Y plane

KEYOPT(6)
Element output:
0 -- Basic element printout
1 -- Also print force-deflection table for each element (only at first iteration of problem)

REFERENCES

[1]. http://www.weitzlux.com/aviation/attorney/learnmore/fatalhelicopterinjury_4325.html.

[2]. J. D. Glatz, “Energy Attenuation for Crashworthy Seating Systems: Past, Present, and Possible Future Development”, SAFE Association (U.S.). Symposium., 1991.

[3]. Stanley P. Desjardins, “The Evolution of Energy Absorption Systems for Crashworthy Helicopter Seats”, American Helicopter Society International, Inc., May 6 2003.

[4]. Paolo Astori, “Numerical Optimization of a Seat Energy Absorber” (http://www.aero.polimi.it/~morandin/Home/ikus4.pdf)

[5]. Simula Inc., “Aircraft Crash Survival Design, Guide Volume 1: Design Criteria and Checklist”, December 1989.

[6]. Raymond W. Mort, “Crashworthy Aircraft Seat”, United States Patent US 6,394,393 B1, May 2002.

[7]. Mr. Richard F. Campbell, "Design of a Crashworthy Crew Seat for the Boeing Vertol Chinook Helicopter", SAFE Association, October 1980.

[8]. Howard A. Lindsay and Stephen M. Motoyama, “The Weight Optimization of an Armored Crashworthy Crewseat Through the Use of Advanced Composites and Design”, NASA Conference Publication, Vol. 1, pp. 103-117, November 1989.

[9]. “Military Specification Seats, Helicopter Cabin, Crashworthy, General Specification For”, MIL-S-85510(AS), September 1996.

[10]. J. F. M. Wiggenraad, “Design, Fabrication, Test and Analysis of a Crashworthy Troop Seat”, European Rotorcraft Forum, September 1997.

[11]. Hamid Kh. Beheshti, “Crashworthiness Evaluations of Composite Foam Materials Used in Aircraft Seats”, Ph.D. Dissertation, Wichita State University, December 2004.

[12]. http://vincentryan.blogspot.com/feeds/posts/default

[13]. Simula Inc., “Volume II - Aircraft Design Crash Impact Conditions and Human Tolerance”, Aviation Applied Technology Directorate US Army Aviation Research and Technology Activity (AVSCOM), December 1989.

[14]. Gary L. Farley, “Relationship between Mechanical-Property Energy-Absorption Trends for Composite Tubes”, NASA Technical Paper, December 1992.

[15]. Nathan Daniel Flesher, “Crash Energy Absorption of Braided Composite Tubes”, Ph.D. Dissertation, Stanford University, December 2005.

[16]. Henry E. Wilson, James D., “Composite Fibrous Tube Energy Absorber”, United States Patent 4,336,868, Jan 29, 1982.

[17]. John H. Bickford, “Introduction to the Design and Behavior of Bolted Joints”, Taylor and Francis Group, 2008.

[18]. Kiyokazu Seo, Yoshihiro Hayashi, “Webbing for use in Seat Belts”, United States Patent 3,756,288, September 4, 1973.

[19]. www.ansys.com

[20]. http://www.padtinc.com/epubs/focus/common/focus.asp?I=8&P=article2.htm

[21]. Ajaykumar Menon, “Structural Optimization Using ANSYS and Regulated Multiquadric Response Surface Model”, December 2005.

[22]. Anthony A. Giunta, "Overview of Modern Design of Experiment Methods for Computational Simulations", AIAA 2003-0649.

BIOGRAPHICAL INFORMATION

Nauman Mhaskar was born in Ratnagiri, Maharashtra, India in 1983. He received his Bachelor's degree in Mechanical Engineering from the University of Mumbai, India in 2005 and his Master of Science in Mechanical Engineering from the University of Texas at Arlington in 2008. His research interests include mechanical and structural design and analysis, finite element analysis, structural dynamics and various other fields where these principles can be applied.